Methamphetamine detection using nanoparticle-based biosensors: A comprehensive review

Kartikay Lal, Frazer Noble, Khalid Mahmood Arif [*]

School of Food and Advanced Technology, Massey University, Auckland 0632, New Zealand

ARTICLE INFO

ABSTRACT

Drug abuse is a global issue, requiring diverse techniques for recognition of drug of interest. One such illicit drug that is abused worldwide is Methamphetamine (METH). It is an addictive and illicit substance that severely affects the central nervous system. Similar to many other illicit substances, recognition of METH in biological fluids and in more diverse matrices such as wastewater, is a topic of great interest to the government and law enforcement agencies. With the rise of nanotechnology that relies on exploiting the properties of certain materials at a scale down to their nanometer range in conjunction with aptamers, molecularly imprinted polymers as well as antibodies have gained much attention over the last decade. The scope and appositeness of nanomaterials have significant characteristics that are highly suitable for recognition of illicit chemical compounds such as METH. This comprehensive review focuses on the detection of METH using nanoparticles in real world samples such as biological fluids and wastewater, while discussing varieties of materials used as nanoparticles and that aid in its recognition. It also offers insights into future opportunities and challenges that come with the use of nanotechnology in sensing applications.

1. Introduction

Methamphetamine (METH) is the second most abused drug after Cannabis [1,2]. It is illegally synthesized in clandestine laboratories using methods that change overtime with the use of primary precursor chemicals such as ephedrine, pseudoephedrine and phenyl-2-propanone [3]. METH is released into the community and trafficked to various parts of our society through sites like parks, alley ways and even our schools [4,5]. METH is illegally consumed through forms of intake such as pills that are taken orally, in the form of powder that is inhaled, powder mixed with some solution which is then injected into the blood stream or even rolled as a joint and smoked [6]. METH blocks receptors like serotonin and dopamine in the brain, causing erratic behavior. The adverse effects of drug consumption depends on the type of drug and the way it is administered into the human body [7]. However, taking high doses of this illicit substance leads to confusion, disruption of alertness and paranoia. More lethal consequences include rapid heart rate, stroke and even death [8,9]. In some cases, however, METH is prescribed by medical professionals in very small quantities and administered within controlled conditions that aids in treating disorders such as narcolepsy, hyperactivity disorder and in some instances, even excessive obesity

[10]. A report released in 2015 by the United Nations Office on Drugs and Crime reveals that METH or amphetamine-type stimulants (ATS) production amoutns to nearly 500 metric tons a year, with over 24.7 million abusers worldwide, incurring billions of dollars of socioeconomic damage [11,12]. To control the spread of this illicit and harmful substance, many studies have been carried out efficiently to identify trace amounts of METH and other forms of ATS in biological samples including water samples from wastewater treatment plants (WWTP).

Collection of samples such as various bodily fluids and water from WWTP are common sources for detection of illicit substances that are consumed by humans. Therefore, it would be helpful to understand how these substances enter the human body which gets processed by various organs and biological processes and then excreted through various mediums [13]. The absorption of drugs by the human system, distributing, metabolizing the drugs and excretion is called Pharmacokinetics [14] and it shows the journey of drugs from intake to the destination. The first phase involves the procedure of consuming the illicit substances known as the absorption phase. The various mediums of this phase are oral intake, such as smoking and eating; inhalation, such as snorting; and injection, like injecting drugs into the blood stream. The

second phase is the distribution stage which involves the drugs or substances going through the human metabolism like hepatic (liver) if ingested and stomach, lungs, and gut (intestinal) if smoked and snorted. The final stage involves drug metabolites being secreted either as unaltered form and/or as metabolites through various human excretes, such as sweat, oral fluid, blood (plasma) and urine [15–17] and the flow of illicit compounds that are byproducts of illicit substances flow from the body to the point of sample collection. Fig. 1 pictorially represents the process of metabolites entering wastewater.

As mentioned before, there are various methods of administering substances of abuse. Not all drugs are consumed the same way. For example, METH can be administered intranasally as well as intravenously. When a substance is absorbed by the human body by any method of intake, human metabolism breaks down the chemical compounds that are present in drugs and creates by-products. These by-products are known as metabolites that are unique to the drug. Research shows that regardless of the method of intake, the human metabolism generates the same metabolite for a drug [18]. After drug consumption, metabolites are excreted through various forms of biofluids. When METH enters the human body, it generates three metabolites known as Para-hydroxymethamphetamine (p-OHMA), p-hydroxylation and Amphetamine (AMP) with AMP being the most prominent [19].

Literature has presented various analytical approaches for detection of METH and/or metabolites in biofluids such as urine and plasma as well as wastewater chromatography techniques such as gas chromatography (GC) [20–25], liquid chromatography (LC) [26–28] and high performance liquid chromatography (HPLC) [29–35] are popular and conventional techniques that are able to detect low concentrations of METH and its byproducts in urine sample. These techniques when combined with mass spectrometry (MS) such as GC–MS, LC-MS, LC-MS-

MS, yields very low detection levels. Furthermore, thin layer chromatography (TLC) is another variant of the chromatography suite that has been coupled with techniques like fluorescence and HPLC that has been utilized to detect METH in its unaltered form [36–38]. Apart from for the chromatographic techniques, methods like capillary electrophoresis (CE) [39,40] have also reported high sensitivity with accurate results for recognition of METH. Although these traditional methods are relevant for recognition of METH in urine samples, there are some drawbacks such as extensive sample preparation which is time consuming, use of expensive laboratory equipment and the need for trained personnel to operate specialized equipment. However, there are other methods that have also gained much attention such as electrochemical, spectroscopic methods as well as some optical methods.

Compared to conventional methods for detecting METH, biosensors are seen as potential alternatives to overcome the limitation of traditional techniques. Biosensors are composed of biological receptors that allow binding with analytes of interest to the recognition element which can broadly be categorized as DNA [41,42], enzyme [43–45] and antibody [46–48] based elements. Recognition elements such as aptamer that are single stranded DNA are often denoted as aptamer sensor or apta-sensor that can generate an optical, electrochemical, or other signal in presence of a target such as METH. With the use of nanotechnology, the performance of biosensors can be improved which could enhance selectivity, sensitivity, and adaptability of the sensor. The use of nanomaterials has enabled sensors to produce results rapidly with attributes like reproducibility and reduce/eliminate the use of sophisticated and costly equipment [49].

The motivation of this review is to present analytical methods that have been used in amalgam with nanoparticles of various materials for the detection of METH in water. The relevant research articles for the
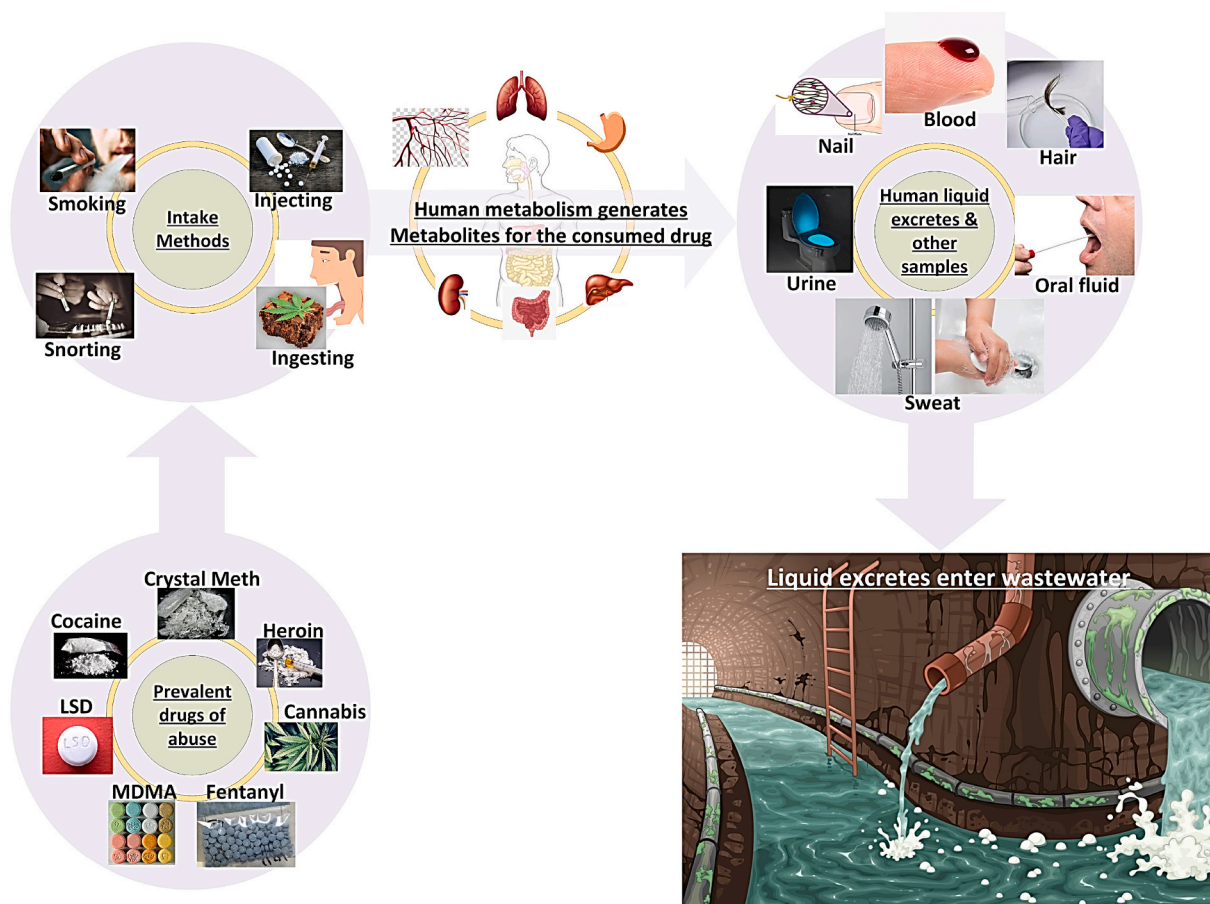

Fig. 1. Drug pathway depicting the process of metabolites entering wastewater.

review were searched using the keyword "nanoparticles" on the biggest journal/article database Google Scholar, that resulted in a few million results from different fields. However, to reduce the number of results, the search terms were refined to more specific keywords such as "Methamphetamine", "gold nanoparticles", "AuNP", "silver nano-particle", "AgNP", "magnetic nanoparticles", "electrochemical", "wastewater", etc. Many combinations of the keywords were also used to find relevant literature that focused on detection of METH in mediums such as water, wastewater, urine, and saliva. The search was performed in the titles and main text of the articles and the articles were mainly selected from Q1 and Q2 ranked journals.

The rest of the paper comprises of two sections. Section 2 dives into the relevant techniques, enumerated by various nanoparticles such as gold, silver, magnetic and more. That are combined with analytical detection techniques such electrochemical, colorimetric, optical, and more. Section 3 discusses the current performance of various methods of detection with an outlook into the future development/improvements of the discussed methods.

2. Recent developments

Nanoparticles are microscopic solid particles that range from 1 to 100 nm. Although nanoparticles are too small to be seen with bare eyes, they exhibit significant physical and chemical properties compared to their larger material counterpart [50]. The surface area to volume ratio for various materials made of nanoparticles possess unique effect on the properties of the material. Nanoparticles enhance the sensitivity of the sensing layer due to the larger surface area that it collectively provides compared to the larger surface area of the same volume of material made up of bigger particles [51]. Many studies have been carried out with

nanoparticles that are made of various materials such as Gold, Silver, Silica, Iron (III) oxide and so on. Fig. 2 shows a range of nanoparticles that have been studied, combined with detection methods that are used to recognize METH in various matrices.

2.1. Gold nanoparticles (AuNPs)

Gold nanoparticles present interesting chemical and physical properties such as chemical stability, unusual optical properties, self-aggregation, and ease of integration with electrochemistry. AuNPs were first synthesized by treating hydrogen tetrachloroaurate with citric acid in boiling water. The method was further developed by changing the gold-to-citrate ratio to control the size of particles [52]. The size of the AuNPs can be synthesized to be in the range of 10–100 nm. It has also been reported that AuNPs can display distinct electronic and optical properties compared to the bulk form [53].

2.1.1. Colorimetric detection

Gold is synthesized in various sizes and shapes at a nanometer scale with different structures such as nanorods, nanoprisms, nanoshells and nanoparticles, each with unique physical and electrical properties that are suitable for specific applications such as x-ray imaging, drug delivery, biosensing and more [54,55]. Furthermore, AuNPs in the field of biosensing provide unique properties such as ease of synthetic manipulation, high X-ray absorption coefficient, provide control over the particle's physio-chemical properties [56], strong binding affinity and adaptable optical properties [57]. One of the major applications of AuNPs is in chemical analysis and biosensing. The techniques that work well with AuNPs can be fluorescence-based, colorimetric, electrochemical, surface enhanced Raman spectroscopy, quartz crystal
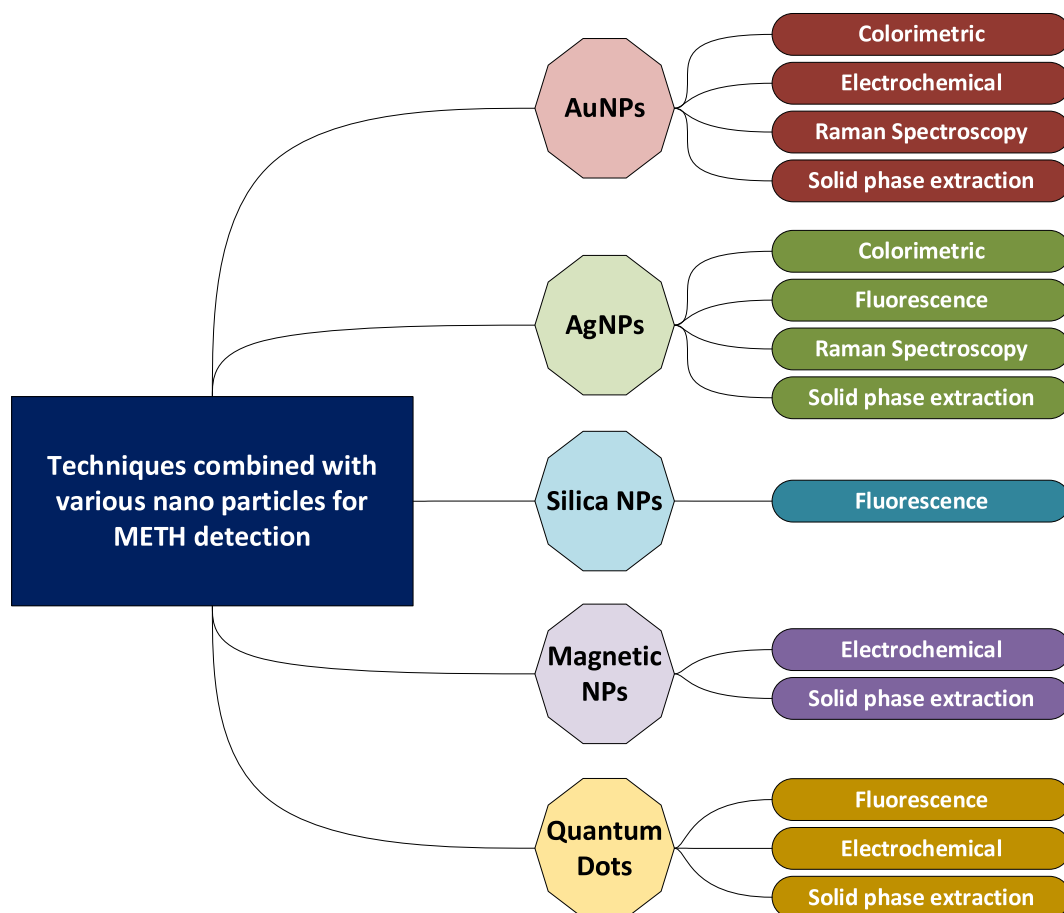

Fig. 2. Detection techniques combined with different nanoparticles for recognition of METH.

microbalance-based and bioassays [58]. AuNPs have been studied for many decades for recognition of certain metals and chemical compounds and METH is one such chemical substance. Recognition of METH with AuNPs provide effects such as apparent changes in color, deflection of light, variations in electrical conductivity and so on. primarily in water or human biofluids.

Research conducted by Shi et al. [59] for recognition of METH in human urine sample was based on the use of a specific aptamer which would bind with METH along with unmodified AuNPs used as indicators. The method is based on the colorimetric approach and with the presence of AuNPs, the sample changes color from red to blue in presence of METH. AuNPs allow for sensitive detection of METH with a detection limit of 0.82 μM and approximately 20 min of reaction time. As stated in their research, METH that was detected in urine could be quantified by change in color of the solution and by measurement of the absorbance ratios at 660 and 525 nm, respectively. The authors also stated that salt was a key ingredient for aggregation of AuNPs. Because of the nature of gold nanoparticles and the presence of nitrogen atoms within the single-strand DNA (ssDNA) gave aptamer the ability to easily attach to the surface of AuNPs, thereby resistance due to salt-induced aggregation is increased. However, when METH is introduced into the solution, its chemical composition disrupts the stabilization effect of aptamer and result in distinct color change to blue because the aptamer favors the presence of chemical compounds present in METH through forming the so called G-quartets, which prevents the exposure of DNA bases to AuNPs due to its rigid structure as also stated in [60]. Since color change signifies the presence of METH which can be clearly observed for qualitative analysis, a spectrometer could also be used for quantitative analysis.

Similarly, Yarbakht et al. [61] studied colorimetric method using AuNPs for detection of METH. The effect of AuNPs and aptamers with added phosphate buffered saline (PBS) for aggregation of nanoparticles for visual detection of METH and 3,4-methylenedioxy-*N*-methyl-amphetamine (MDMA), as both relate to the family of ATS. They began by studying the effects of PBS (salt base with pH of 8) to disperse AuNPs, causing electrostatic repulsion between particles to decrease, resulting in accumulation of AuNPs producing a change in color of solution to purple. Yarbakht and team also indicated that the structure that is formed as a result of METH and aptamer amalgamation does not possess enough affinity to AuNPs, therefore, the particles fail to aggregate. It is only after increasing the concentration of METH in the solution, the apparent change in color of the AuNPs start to appear proving an increase in the aggregation of nanoparticles, which suggests a decrease in the absorbance of AuNPs at 520 nm. A successful detection of METH was observed with a visible change in color at 5 mM of METH in the solution which equates to 7.5 ng/mL within 30 min. It was also reported that MDMA when introduced with the aptamer inflict a slight yet insignificant change in color (and the corresponding absorbance at 520 nm as induced by METH) which indicated that the aptamer was not exclusive to METH and could also interact with other ATS, though with lower affinity.

Furthermore, Mao et al. [62] reported a swift biosensor for recognition of METH and cocaine that is based on the colorimetric detection technique in a single assay. AuNPs and Au@Ag (Au-silver) NPs were functionalized with DNA reporter probes (RP) with wastewater as the sample matrix. RPs comprised of AuNPs, and Au@Ag NPs conjugated with a DNA sequence which is partially paired to the aptamer while capture probes (CP) were prepared using carboxyl coated magnetic beads (MB) conjugated with DNA that are triggered by an external magnetic field. RP and CP both involved extensive preparation taking a few days to produce. The aptamer binds the two CP and RP probes that form a sandwich structure of double-stranded DNA. However, due to high affinity between aptamer and METH, the sandwich structure gets breaks down when the drug is introduced into the solution, leading to color change of the supernatant. It was also reported that a UV–vis spectrometer was used to measure the signal peaks of AuNPs and

Au@Ag that came out to be 520 nm and 400 nm, respectively. It was also found that the surface plasmon resonance frequencies of AuNPs and Au@Ag were quite different even though they had the same particle size. The quantification of the illicit substance in the solution was determined when an external magnetic field was introduced which removed the sandwich structure from the solution, which lead to a decrease in the absorbance intensity. This was then correlated with the concentration of the illicit substance, enabling the quantification of drugs in the solution. Mao and the team were successful in detecting METH from with concentration from 0 to 200 nM and Cocaine from 0 to 150 nM.

Moreover, Adegoke et al. [63] reported on development of graphene oxide (GO)- multi-shaped cetyltrimethylammonium bromide gold nanoparticles (CTAB-AuNPs) with DNA aptamer based colorimetric biosensor for detection of amphetamine (AMP) and METH with hemin as the catalytic signal amplifier. Hemin is a DNA based artificial enzyme which is occasionally used with biosensors because of its catalytic property [64,65]. It was reported that CTAB-AuNPs were first bound to GO through the process of electrostatic interaction which formed a hybrid nanozyme of Go-CTAG-AuNP. The DNA aptamer specific to METH was further bound to this nanozyme surface to capture METH which was followed by binding of hemin to generate a deep blue color, specific to METH. It was also reported that as the concentration of GO increased, the intensity of the surface plasmon resonance absorption peak decreased. Fig. 3 depicts colorimetric process of quantifying the concentration levels of METH in a solution.

2.1.2. Electrochemical detection

As seen from the review so far, colorimetric technique has been widely used for recognition of METH which considers changes in color as the detection mechanism. However, there techniques that analyze changes in electrical conductivity. Electrochemical is such technique that detects small variations in electrical properties of conductors such as changes in current, voltage, resistance, or capacitance [66]. Electrochemical method makes use of electrodes that are fabricated from metals with low oxidative yet high conductive property. Due to this reason, gold and silver and few other metals are commonly used for fabrication of electrodes. Iridium is one such element which was used as a compound with tin for fabrication of minuscule electrodes. Performance of Iridium-tin-oxide (ITO) was studied by Yeh et al. [67], who developed an immunoassay method that used electro-microchip to detect an immune-reaction signal in presence of METH in urine samples. Their method consisted of six parallel ITO electrodes on a glass slide and a circular reaction well. Two parallel electrodes had 20 μm separation between them, and the electrode length was 1500 μm with a reaction well bonded on top of the electrodes using polydimethylsiloxane (PDMS) that formed a well with a fixed volume of 30 μL. The surface was altered on the glass slide from methyl group to the aldehyde functional group using self-assembled monolayer (SAM) method. This was further followed by an injection into the electro-microchip with anti-METH antibody colloidal gold conjugate solution, which was mixed with the sample for 1 min, that allowed residual anti-MET-antibody-colloidal gold conjugates to bind with Bovine Serum Albumin (BSA)-MET conjugates. The changes in impedance that occurred as a result of reaction between two parallel electrodes, a LCR meter was used to make the measurements. This change in impedance equated to a detection limit of 50 ng/mL of METH in a sample of urine.

On the other hand, Alijanianzadeh et al. [68] took a different approach to design a nano-biosensor with FT-IR method, and the results of the method were evaluated using cyclic voltammetry. The method designed to detect METH by coating polycarbonate surface with AuNPs and anti-methamphetamine aptamer. Anti-methamphetamine DNA aptamer was constructed with 20 nucleotides poly adenine. Recognition of METH at different concentrations were studied by spectral changes after binding of the aptameric sequence to AuNPs of size 30 nm were coated on top of a polycarbonate surface and binding of METH to
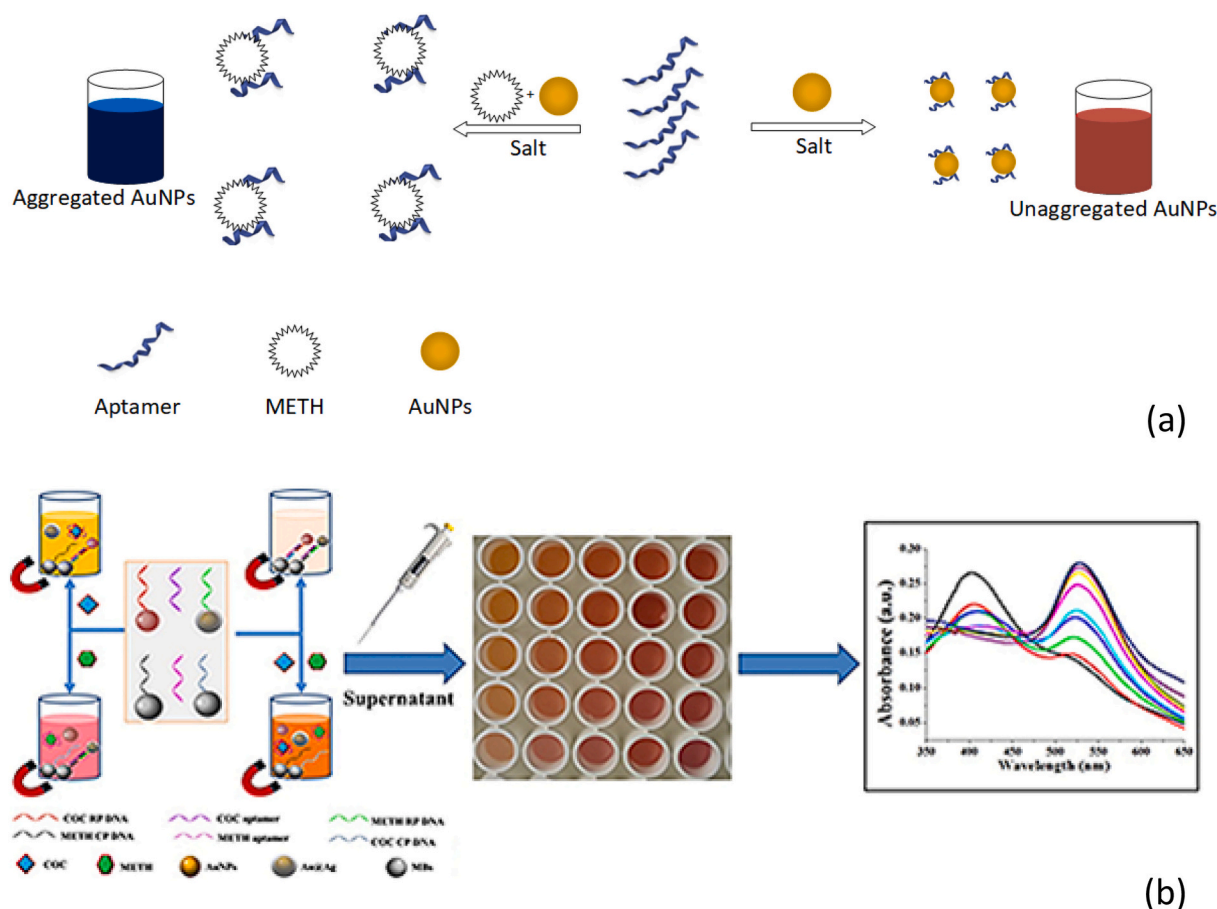
Fig. 3. Depiction of the operation of different biosensors for detection of METH in urine samples. (a) [59], (b) [62]

aptameric sequence. The reaction of METH with the biosensor yielded a detection limit of 2 μM. The result of FT-IR approach was then evaluated by electrochemical method. This sensor comprised of three electrode carbon cells that were used to perform cyclic voltametric measurements. The working electrode was modified glass electrode, the reference electrode was selected to be made of Ag/AgCl, and the counter electrode was fabricated from platinum. When all the potentials were calculated against the silver (Ag) electrode it was found that aptameric sequence that was bound on surface of gold-coated polycarbonate, the reflection intensity from UV–Vis-IR spectroscopy decreased by 8%. The study found a decrease in intensity of reflection which was directly proportional to an increase in concentration of METH after incubation with different concentrations. The voltametric method yielded a detection limit of 5 μM.

Furthermore, Ebrahimi et al. [69] made use of METH specific aptamer with AuNPs using electrochemical impedance spectroscopy (EIS) as the detection technique. Impedimetric measurements were taken using a standard three-electrode electrochemical system which included AuNPs/METH and AMP aptamer modified working electrode, counter electrode made of platinum and Ag/AgCl/KCL saturated reference electrode. The synthesized AuNPs were characterized by UV-VIS spectroscopy with an average diameter determined to be 16 nm. Using the technology known as Systematic Evolution of Ligands by Exponential (SELEX), a single stranded DNA (ssDNA) aptamer specific to METH was developed by Ebrahimi and the team which would fold and unfold in the presence of METH and AMP which led to the fluctuations in impedance measurement. AuNPs played a key role of binding unfolded aptamer with the gold coated electrode. Their study found that the affinity of the aptamer was more towards METH with the folding capability compared to AMP.

A slightly different approach to recognition of METH was taken by Rafiee et al. [70] that studied the performance of electrochemical sensor using screen printed electrodes (SPE) that were modified with AuNPs/multiwalled carbon nanotubes (MWCNT)-Nafion (Nf). The concentration level of METH was determined by square wave anodic stripping voltammetry (SWASV) in alkaline media. Experimentation indicated that the current flow at the bare screen-printed carbon electrodes and SPE modified with MWCNT-Nf were negligible. However, in the presence of AuNPs at the modified layer, the oxidation current increased considerably resulting in a distinctive oxidation peak which could be observed at about 280 mV potential. It was also reported that CNTs themselves could be considered as a high area support, but the electroactivity arises solely from the AuNPs. The results indicated the sharpest and highest signal for 0.1 mM of METH solution. This is due to MWCNT-Nf/AuNPs nanocomposites that benefit from specific affinity to nitrogen and fast electron transfer rate of MWCNTs as nanomaterials exhibit special physicochemical properties which helps to improve the sensitivity and selectivity of stripping voltametric techniques.

Moreover, Maryam et al. [71] studied the use of unmodified and modified glassy carbon electrode (GCE) for recognition of METH. The GCE was modified with MWCNT with AuNPs that were linked to nanomagnetic core shells. They chose cyclic voltammetry to carry out determination of METH in various pH levels ranging from 3 to 12 with modified GCE in human urine samples which were spiked with different concentrations of METH. It was found that the peak potential of METH was undetectable with pH levels in the range of 3 to 7.5. However, the peak potential of the modified GCE changed to negative values as pH of the solution was increased from 8 to 12. Thereafter, square-wave voltammetry (SWV) method was used for determination of METH using modified GCE with the electrolyte at pH of 10.5 and 150 μL 0.1 M of

NaCl. An increase in the response from SWV was noticed upon addition of METH to the buffer solution.

2.1.3. Raman spectroscopy

The studies discussed above, underwent extensive pretreatment of electrode and aptamer preparation that changes the nature of the sample or destroys it. Another technique which is widely used for detection of substances in liquid form is Raman spectroscopy (RS). This technique utilizes the interaction of light with the chemical bonds within a material. This non-destructive technique provides detailed chemical structure and molecular interactions [72,73]. Just like other detection techniques, RS has over 25 variants that enhances its performance such as surface-enhanced Raman scattering (SERS), Fourier transform Raman scattering (FTRS), hyper-Raman scattering, tip-enhanced Raman scattering (TERS), just to name a few [74]. For recognition of METH, SERS has been found to be most prevalent variant that is combined with AuNPs. Ma et al. [75] developed a SERS platform through self-assembly of AuNP arrays at the cyclohexane/water interface to detect METH in human urine. AuNPs formed a thin layer on the surface of the sample solution. AuNPs were self-assembled with a suitable balance of various forces which ensured that the nanoparticles not only aggregate but instead formed a close-packed array at the surface of the sample. This layer of nanoparticles helped trap drug molecules in between individual particles and with time, the morphology of the assembled AuNPs grew from a few nanometers to few micrometers and therefore, these interparticle gaps led to a significant enhancement in Raman signal. UV–vis absorbance spectra showed a surface plasmon resonance of around 660 nm that is red-shifted by 140 nm compared to 520 nm of AuNP colloids which indicated a strong interparticle plasmonic coupling between individual AuNPs. Their developed method was able to recognize a concentration of 1 ppm (parts per million) of METH.

Hong et al. [76] took a slightly different approach by utilizing opto-plasmonic combined materials for trace detection of METH analyte. They studied the dielectric effect of silicon nano/microspheres that were placed on top of a monolayer of AuNPs to improve the electric field intensity and develop electromagnetic hot spots. A solution containing analyte was introduced with AuNP colloids followed by addition of cyclohexane that caused AuNPs to self-assemble. Ethanol was then added to the solution which was left to dry resulting in the formation of AuNP monolayer. Furthermore, silicon dioxide (SiO_2) was added to the solution which were in spherical shape with a diameter of 5 μm and

attached itself to the self-assembled AuNP monolayer. The final solution was exposed to SERS for measurement which yielded a low detection concentration of 1 nM. Fig. 4 illustrates the fabrication process of AuNP monolayer and the opto-plasmonic combined interface.

Mao et al. [77] studied the effect of METH analyte with AuNP combined with METH specific aptamer using SERS. Their method was based on aligner mediated cleavage (AMC) of DNA. The AMC hybridized with complementary DNA that resulted in AuNPs to aggregate which generates plasmonic coupling effect. AMC acts as a catalyst in METH recognition which cleaves the aptamer that is not bound to the analyte (METH) which results in the distance of AuNPs linked by DNA to reduced thereby reducing the need for structural changes when the aptamer binds to the ligand and therefore, rhodamine 6G attached to AuNPs help produce an enhanced SERS. This method achieved detection of concentration level of 7 pM. Fig. 5 illustrates how AMC and R6G react in the presence of METH. Few other studies have taken place that use unique properties of AuNPs to detect trace amounts of METH in urine or saliva samples [78–82].

A few advantages of using gold nanoparticles have so far been discussed that are spherical in shape with size that is approximately 30 nm in diameter. However, there other shapes of nanoparticles that differ in properties and color measurements to that of spherical nanoparticles. Although this review focuses on nanoparticles, there are other variants that belong to the realm of nanomaterials such as nanorods that have some similar applications in the field of biosensing. Weng et al. [83], studied the use of gold nanorods (AuNRs) for recognition of METH. They developed a method to detect METH in human urine using chemometric and dynamic SERS (D-SERS) method with Methoxy-Polyethylene glycol (mPED-SH) coated gold nanorods (AuNRs) which yielded a detection level of 0.4, 3 and 30 ppm of MAMP in urine sample with accuracy of 94.5%, 92% and 92.5% respectively. Table 1 summarizes all the studies discussed on gold nanoparticles.

2.2. Silver nanoparticles (AgNPs)

Silver is a noble metal, and its nano sized particles exhibit unique tunable plasmonic properties. The shape and size of the silver nanoparticle allows manipulation of its surface plasmon resonance frequencies as the particle interact with the environment it is in [86]. The particles synthesized from the parent bare metal form exhibit great physical and chemical properties. However, these nanoparticles can be
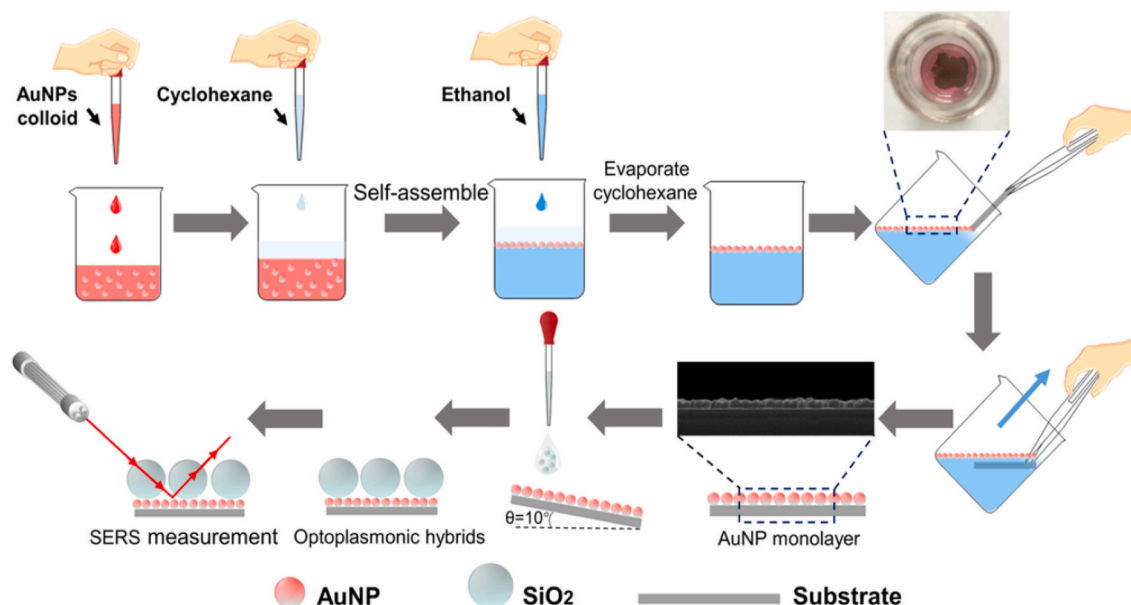

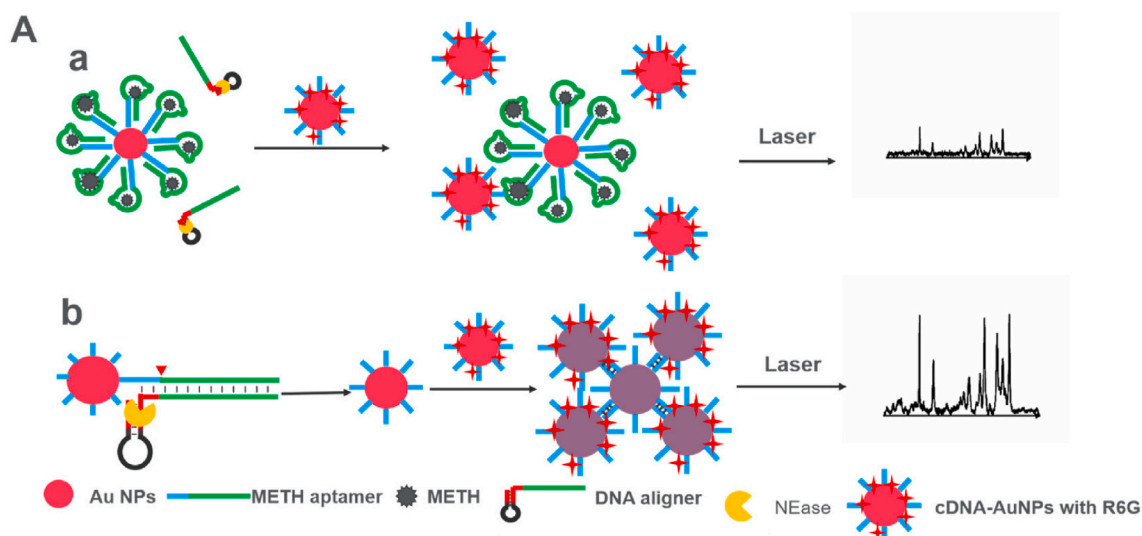**Fig. 4.** Flow diagram for fabrication of AuNPs monolayer [76].

Fig. 5. (a) AMC unable to complete in presence of METH, (b) the formation of DNA-assisted self-assembly of AuNPs in presence of METH [77].

Table 1
Gold nanoparticles-based detection techniques.

Detection technique	Type of Nanoparticle	Limit of Detection	Detection time	Matrix type	Ref
Colorimetric	Unmodified AuNPs	0.82 μM (365 μg/mL)	20 mins	Human urine	[59]
	Unmodified AuNPs	5 mM (2.22 g/mL)	30 mins	–	[61]
	AuNPs + Au@Ag NPs	150 nM (66.75 μg/mL)	60 mins	Wastewater	[62]
	Multi shaped AuNPs	28.6 ng/mL	1 min	Water sample	[63]
Voltammetry	AuNPs	5 μM (2.22 mg/mL)	–	–	[68]
FT-IR	AuNPs	2 μM (890 μg/mL)	–	–	[68]
Electrochemical Impedance spectroscopy	AuNPs	–	–	–	[69]
Square-wave voltammetry	MWCNT-Nf-AuNPs	1.1 μg/mL	–	–	[70]
	MWCNT-AuNPs	16 nM (7.12 μg/mL)	–	Spiked human urine	[71]
SERS	AuNPs	1 ppm (1000 ng/mL)	5 mins	Human urine	[75]
	AuNPs with SiO$_2$	1 nM (445 ng/mL)	–	Human urine and saliva	[76]
	AuNPs with AMC and R6C	7 pM (3 ng/mL)	–	Serum	[77]
	AuNRs	0.4 ppm (400 ng/mL)	2 mins	Human urine	[83]
	AuNRs	500 ng/mL	–	Human urine	[84]
	AuNRs	5 mM (2.22 g/mL)	–	Saliva	[85]
	AuNPs	160 ppb (160 ng/mL)	30 s	Human urine	[78]
Electrochemical	AuNPs	10 nM (4.45 μg/mL)	–	Real sample	[79]
Electrochemical	AuNPs	50 ng/mL	13 mins	Human urine	[67]
Piezoelectric	Gold coated polymer	1 μg/mL	20 mins	Real sample	[80]
Fiber optic particle plasmon resonance	AuNPs	0.16 ng/mL	Real time	Urine sample	[81]
Localized surface plasmon resonance	AuNPs	500 nM (225.5 μg/mL)	–	–	[82]

enhanced to suit the application by coating another metal around it such as gold [87]. An image taken with a transmission electron microscope (TEM) is shown in Fig. 6.

Salemmilani et al. [89] studied effect of AgNPs modified with iodide using an electrode integrated microfluidic approach with detection carried out by SERS method. It was reported that METH molecules have low affinity to AgNPs. It was also reported that uncapped AgNPs are thermodynamically unstable and aggregate soon after synthesis. Thus, capping agents are used to stabilize AgNPs but have undesirable consequences with SERS spectrum due to the interference of capping agents with the analyte, especially at low analyte concentration levels. As AuNPs were sourced which were precoated with citrate. Citrate was stated to interfere with spectroscopic measurements and hence, the nanoparticles were modified with sodium iodide to separate citrate from them. A principal component analysis (PCA) model was incorporated to compute positive detected results from negative results. SERS spectra revealed peaks at around 1004, 1030 and 1600 cm^{-1} in the presence of METH in saliva.

Another microfluidic approach was taken by Andreou et al. [90] to detect METH in saliva. The microfluidic channels were designed in such
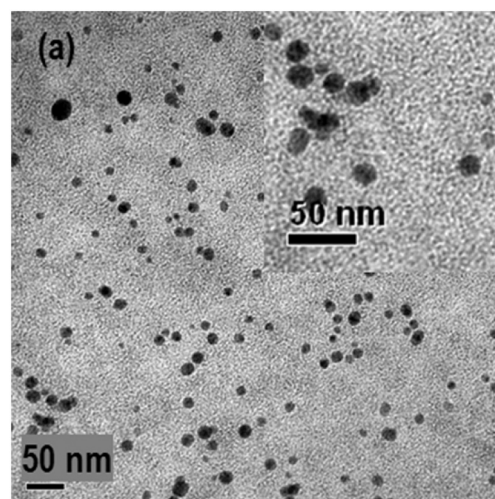

Fig. 6. TEM image of AgNPs in Agar [88].

a way that allowed the analyte to diffuse with AgNPs first. The METH molecules introduced into the microfluidic steam containing AgNPs, on which the METH molecules were adsorbed. Any larger species that maybe present in the sample diffuse more slowly, and hence, a partial separation of METH molecules from the complex fluid was accomplished. It is known that METH does not have strong affinity for silver and therefore does not support aggregation of AgNPs reliably. Salt served as a catalyst for AgNPs to aggregate, which resulted in strong SERS signals. In the stream of AgNPs where METH molecules could reach by diffusion, SERS spectra were observed at peaks of 1004, 1030, 1219 and 1600 cm^{-1} with detection limit of METH reached at 100 nM.

A study using SERS detection technique but using AgNPs on agarose gel (AgNPs/Agar) for detection of METH on latent fingerprints was carried out by Souza et al. [88]. It was reported that AgNPs/Agar substrate was suitable for SERS-active substrate for detection of METH. A film of AgNPs/Agar was deposited on aluminium slide to perform fingerprint tests. Their results show that the SERS spectra of METH gathered on surface of AgNPs are different to those of METH water solution. The gathered METH molecules on AgNPs were detected at concentration level of 1×10^{-5} mol/L.

So far, applications of gold and silver nanoparticles for recognition of METH have been discussed with AuNPs being able to disperse more uniformly with homogeneous particle size. There are other nanoparticles such as magnetic, silica and iron (III) oxide that have been used for METH recognition. But there is also a blend of gold and silver nanoparticles, spherical shaped particles with gold at the center of a silver outer shell. Literature reported that AgNPs produce better SERS signals compared to AuNPs. It was also reported that the Au@Ag NPs are capable of producing high Raman enhancement compared to its larger AgNPs counterpart [91]. Mao et al. [92] has conducted many studies involving the use of different types of nanoparticles. One such study investigates the effects of Au@Ag NPs, for recognition of METH using SERS in spiked human urine samples. AuNPs exhibit an absorbance band at 520 nm which is visible as a red solution. However, a shift from red to yellow is observed for Au@Ag NPs. The formation of AuNPs and Au@Ag is indicated by a shift of new bands at 510 nm and 400 nm indicating that they have different surface plasmon resonance frequencies despite the same particle size of approximately 40 nm. For recognition, a DNA aptamer as the biological receptor was used which detected a Raman signal of 4-mercaptobenzoid acid (4-MBA) enhanced by Au@Ag core-shell. 4-MBA and METH aptamer served as a SERS donor by being absorbed on Au@Ag. When METH was added to the homogeneous Raman labelled Au@Ag, the aptamer got displaced from the surface of Au@Ag which subsequently led to aggregation of Au@Ag. Corresponding volume of aptamer was displaced from the surface of Au@Ag when different concentrations of METH were added to the solution. When increasing concentration levels from 1 to 10 μM of MBA were added, the Raman signal intensity of 4-MBA changed considerably. Raman peaks were observed at 1588 cm^{-1} when METH was introduced. The signal increased significantly with increasing concentration levels of METH from 0.5 to 50 ppb owing to the increasing hot spots.

Using Au@Ag core-shell Mao et al. [93] conducted another study by using the colorimetric technique to detect METH and cocaine using non-aggregated Au@Ag core-shell NPs. The biosensor consisted of a reporter probe (RP) which was derived by modifying Au@Ag core-shell NPs with a DNA sequence which was partially complementary to the aptamer. The capture probe (CP) was super paramagnetic beads (MB) with a carboxyl-modified coating, which were conjugated with the CP DNA. The concentration of MB causes the change in ratio between CP and RP, which impacts the sensitivity of the assay significantly. The probes were tested in spike samples of urine with METH and cocaine. Their experimental results show a significant change in color from red to yellow between AuNPs and Au@Ag which can be observed with the naked eye. The average diameter of the Au@Ag core-shell NPs was measured to be approximately 40 nm and the experiments showed that the aptamer could bind to the RP and CP to form Au@Ag-DNA-MBs sandwich

structure through hybridization. After the complex sandwich structure is formed, the solution is exposed to an external magnetic field which helps to remove the sample structure from suspended state, which in-turn reduces the intensity of surface plasmon resonance (SPR) signal from Au@Ag core-shell NPs. However, the aptamer binding to two probes is prevented when target drug is introduced into the solution. Au@Ag-DNA-MBs complex is incapable to form, thus due to high affinity of the aptamer, it is successfully able to bind with target drug molecules. Different concentrations of METH were introduced into the sample ranging from 0 to 200 nM which showed a color change of the supernatant solution from light yellow to deep yellow as the concentration of METH was increased. The peak SPR signal was observed to be proportional to increasing METH concentration which led to the deformation of Au@Ag-DNA-MBs sandwich structure. Hence, the linear range was determined from 0.5 to 200 nM with a limit of detection of 0.1 nM. Fig. 7 depicts the experimental process carried out for this research.

Mao et al. [94] conducted another study for recognition of METH in wastewater using SERS which is focuses on the fabrication of Au@Ag core-shell nanoparticles on nanofibrous paper matrix. The process is illustrated in Fig. 8. The fibrous paper was altered with synthesized Au@Ag core-shells and functionalized with poly-L-lysine (pLL) which enabled strong SERS signal. Au@Ag were attached on to a paper matrix by exploiting positively charged amine functional groups and pLL's low Raman scattering cross-section. This acted as a catalyst for ionic equilibrium of negatively charged Au@Ag on the glassy paper. METH was spiked in the sample solution with 2 μL of standard concentrations with logarithmic increments (0.01, 0.1, 1.0, 10.0, 100.0, 1000.0 and 10,000.0 ppb). Different concentrations of METH were analyzed using Raman spectra and the results indicated an increase in the intensity of the signal when METH concentrations were logarithmically increased from 10^{-1} ppb to 10^4 ppb with the limit of detection estimated to be 7.2 ppt (parts per trillion).

Another study conducted by Kline et al. [95] who developed a microfluidic platform to investigate various aspects such as material of nanoparticle, size of nanoparticle, excitation wavelength, capping agents and various drug concentration levels achievable using Au and Ag nanoparticles for detection of various illicit substances including METH. For their application, the ideal sizes for AuNPs and AgNPs were found to be 60 nm and 50 nm, respectively. Their results show that gold with borate capping agent is the best performing nanoparticle material. It was reported to provide a background with the analyte that did not interfere with the signal which was successfully dispersed in the presence of analyte molecules. The limit of detection of METH was measured to be between 4.5 ng/mL and 13 ng/mL. A summary of various detection techniques that have incorporated Au@Ag nanoparticles have been presented in Table 2. An image from scanning electron microscope (SEM) of Au@Ag core-shell nanoparticles is shown in Fig. 9. UV–vis spectra of Au@Ag and AuNPs is also shown in this figure.

2.3. Magnetic Nanoparticles (MNPs)

Gold and Silver nanoparticles have been used in abundance for detection of METH as well as other drugs/molecules of interest that have facilitated in the detection process. Magnetic nanoparticles (MNP) have also been used to detect molecules primarily with phase extraction process. For METH detection, MNPs have commonly been integrated with lateral flow immunoassays (LFIA) as well electrochemical detection technique. Riahifar et al. [96] introduced a METH detection method based on modified glassy carbon electrode (GCE) using Fe_3O_4@PPy core-shell along with electrochemically reduced graphene oxide (ErGO) in urine samples. Electrode was first modified using graphene-based nanocomposites because ErGO can be reduced electrochemically which results in high electrical conductivity compared to generic graphene oxide (GO). GO was casted on the GCE surface and its electrochemical reduction of Fe_3O_4@PPy core-shell was casted on ErGO/GCE. The analysis for METH detection were based on the collective effects of
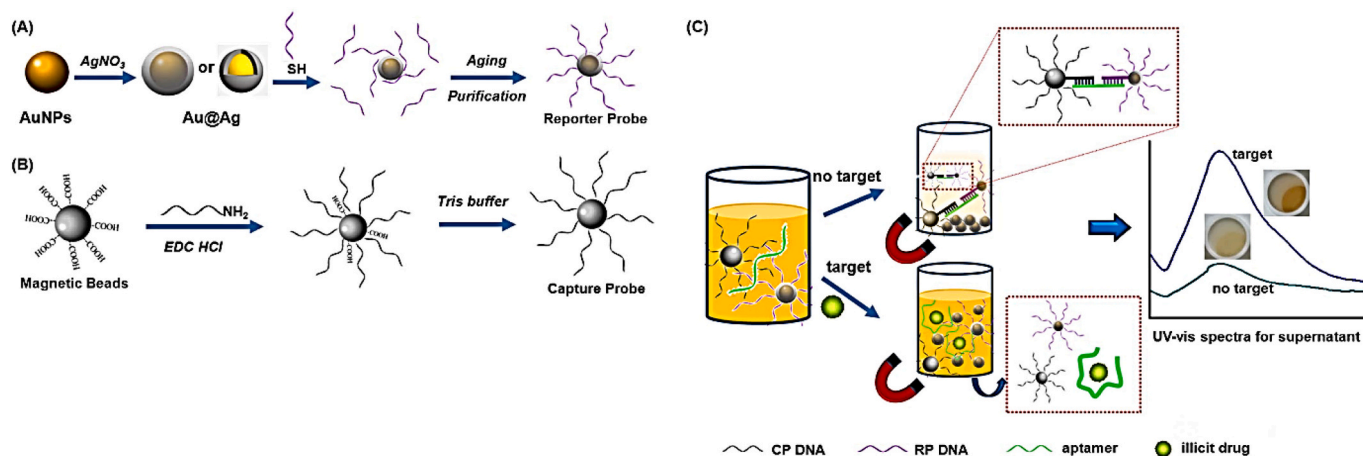
Fig. 7. Illustration of preparation of RP (A), CP (B) and colorimetric detection of METH based on non-aggregation of Au@Ag core-shell NPs (C) [93].
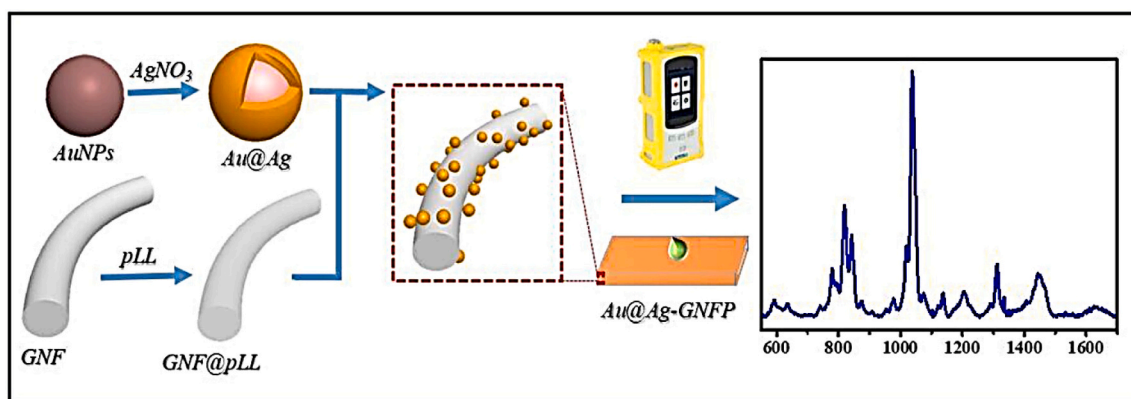

Fig. 8. Schematic illustration of the aggregation of Au@Ag on a glass nanofibrous paper SERS substrate [94].

Table 2
Gold-Silver core-shell nanoparticle-based detection techniques.

Detection technique	Type of Nanoparticle	Limit of Detection	Detection time	Matrix type	Ref
SERS	AgNPs	–	2 mins	Saliva	[89]
	AgNPs	10 nM (4.45 μg/mL)	–	Saliva	[90]
	AgNPs/Agar	1×10^{-5} mol/L (10 nM/mL)	–	Latent fingerprint	[88]
	Au@Ag NPs	50 ppb (50 ng/mL)	–	Spiked urine	[92]
	AuNPs and AgNPs	13 ng/mL	–	Spiked water sample	[95]
Colorimetric	Au@Ag-DNA-MBs	200 nM (89 μg/mL)	–	Spiked urine	[93]

GO and core-shell immobilized on the glassy carbon electrode (Fe_3O_4@PPy/ErGO/GCE). Core-shell nanoparticle was characterized by Fourier transform infrared (FT-IR) spectra for Fe_3O_4 with a peak observed at 3400 cm^{-1}. Electrochemical measurements were taken using techniques such as square wave voltammetry (SWV) and cyclic voltammetry (CV) which were applied to the modified electrode that comprised of BR buffer solution with pH of 8. The CV results showed peak current was enhanced after covering the GCE surface by ErGO, indicating ErGO as a highly conductive film. The analyte oxidation signal was significantly increased after casting core-shell on ErGO/GCE electrode with Fe_3O_4@PPy/ErGO/GCE. The limit of detection for METH with Fe_3O_4@PPy/ErGO/GCE sensor using SWV was computed at 1 nM in urine sample.

Haeri et al. [97] carried out a similar approach of using solid phase extraction (MSPE) combined with bio-dispersive liquid-liquid micro-extraction (DLLME) using Fe_3O_4@PPy magnetic nanoparticles (MNPs) for the recognition of METH in human urine sample. Fe_3O_4@PPy MNPs were characterized using Fourier transform infrared spectroscopy (FT-IR) and X-ray diffraction (XrD) methods. The urine samples were prepared and spiked with 50 μg/L of METH and then 30 mg of Fe_3O_4@PPy NPs was added to the solution. After vigorous stirring Fe_3O_4@PPy NPs were separated from the sample solution with an effective magnetic field. The supernatant that was left behind was decanted. Their results indicated a limit of detection of 0.33 μg/L detected within 2 min.

Furthermore, Taghvimi et al. [98] studied the effects of magnetic nanoparticles coated with carbon for stir bar sorptive extraction method for recognition of METH. Urine sample is spiked with 0.1 μg/mL of METH and dipped a homemade stir bar which was stirred at 600 rpm for 10 mins. The sample solution was exposed to an external magnetic field to separate the magnetic nanoparticles (MNP) from the medium and 20 μL of acetone was inserted to the HPLC-UV device. The structure of MNP-solgel stir bar was examined by scanning electron microscope (SEM) and it was found that the MNP were trapped in the surface of stir bar and the solgel matrix. Stir bar was coated uniformly with MNP with an estimate particle size of 35 nm. As for urine samples, it was observed that the characteristics like acidity and alkalinity of the sample played a significant role in the effective interaction between the analyte and the
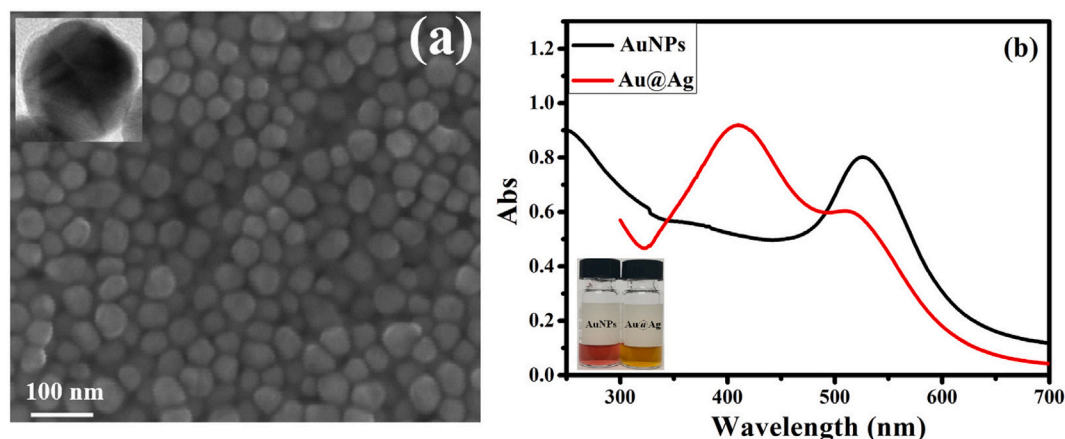
Fig. 9. (a) SEM image of as-prepared Au@Ag core-shell nanoparticles. The inset shows TEM image of a single Au@Ag particle. (b) UV–vis spectra of Au@Ag and AuNPs [92].

MNP solgel coated surface of stir bar. Their method resulted in good linearity with detecting concentration levels of METH between 20 and 2500 ng/mL.

On the other hand, Taghvimi et al. [31] also studied the effects of magnetic nano graphene oxide (MNGO) for recognition of METH using magnetic solid phase extraction technique (MSPE). Nano-graphene oxide (NGO) was synthesized and functionalized using MNPs. Human urine samples were acquired and adjusted to pH of 11 which were spiked with various concentrations of METH. MNGO was utilized as an adsorbent material for extraction of METH which was used for determination and quantification by high performance liquid chromatography – ultraviolet (HPLC-UV). FT-IR spectra was used to characterize and analyze graphene oxide (GO), MNGO and MN with peaks detected at 3447 and 1231 cm^{-1}. These peaks indicate stretching and bending of the O—H bonds in the GO spectra. Another peak was observed at about 619 cm^{-1} that indicated the formation of Fe—O and presence of Fe_3O_4 on GO. The FT-IR spectrum of MNG showed the presence of Fe—O stretching peak at 623 cm^{-1} proving that Fe_3O_4 is attached to the graphene sheet. The results show a good linearity in the range of 100–1500 ng/mL with a limit of detection of 30 ng/mL. Fig. 10 illustrations the procedure of METH extraction using MNGO with MSPE method. Table 3 summarizes all the studies discussed on magnetic nanoparticles. Magnetic nanoparticles were also integrated with bioMEMS for detection of molecules [99].

A point-of-care technique was also studied by Yang et al. [100] that

Table 3
Magnetic nanoparticle-based detection techniques.

Detection technique	Type of Nanoparticle	Limit of Detection	Detection time	Matrix type	Ref
SWV	Fe_3O_4@PPy/ ErGO/GCE	1 nM (445 ng/mL)	–	Urine sample	[96]
DLLME-MSPE	Fe_3O_4@PPy	0.33 μg/L (0.33 ng/ mL)	2 mins	Spiked urine	[97]
Stir-bar sorptive extraction (SBSE)	Carbon coated MNC	2500 ng/ mL	–	Spiked urine	[98]
MSPE	MNGO	30 ng/mL	< 2 mins	Spiked urine	[31]

used a lateral flow immunoassay with a technique called giant magnetic resistance (GMR) to analyte the distribution of magnetic nanoparticles. The LIFA consists of three different pads namely sample, conjugate, and absorbent with a nitrocellulose membrane on a poly vinyl chloride (PVC) substrate. The conjugate pad comprises of the MNP-labelled antibody, while the absorbent pads provide capillary force for the lateral flow of the liquid. The measurements were taken by custom built analogue to digital converter (ADC) and other processes were managed through a microprocessor. Their technique showed a good linear
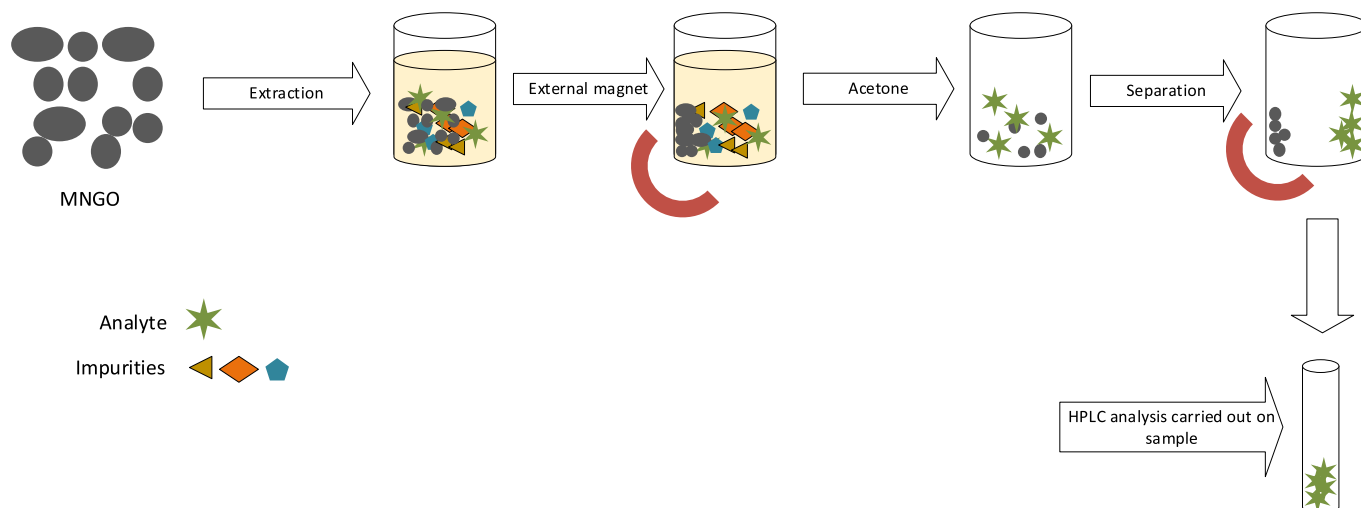

Fig. 10. Illustration of MSPE procedure of METH extraction from spiked urine sample.

performance with a detection limit of 0.1 ng/mL of METH.

2.4. Quantum Dots (QDs)/Carbon Dots (CDs)

CDs have been recognized to be the most proactive members of the nanocarbon group that have a unique photophysical performance that stems from their excitation-wavelength-dependent emission [101]. CDs have cores that comprise of monolayers of nanosized graphene and simple oxidative treatments generate carboxyl and carbonyl groups on CD surface that have been incorporated for recognition of trace amounts of METH [102]. Kim et al. [103] developed a fluorescence-quenching system suitable for detection of METH precursors using amine-functionalized carbon dots. CDs were synthesized through hydrothermal treatment of a mixture of urea and citric acid. The two precursors namely, phenylpropane-1,2-diol (PAC-diol) and phenylpropane-2-one (PSP), were found to quench the fluorescence of aqueous suspension of CDs in such a way that results in linear recognition with the concentration of the precursors. The CDs immobilized on a glass coverslip were able to detect the METH precursors in an aqueous dispersion. Furthermore, PAC-diol had a more effective quenching effect due to its two O—H groups being able to bind more strongly to the CD's surface compared to PSP. It was also reported that the METH metabolite compound named Amphetamine sulphate quenched fluorescence to a small extent, while the common dilutants such as paracetamol, caffeine and sodium chloride were found to have no effect on fluorescence. The theoretical detection limits were calculated to be 2 μg/mL for PAC-diol and 3 μg/mL for PSP.

On the other hand, Mandani et al. [104] studied the effect of molecularly imprinted polymers (MIPs) by using green carbon quantum dots (CQDs) and mesoporous structure imprinting microspheres (SiO$_2$@CQDs@ms-MIPs) for recognition of METH in plasma and urine. While NIPs (SiO$_2$@CQDs@ms-NIPs) were synthesized, the particle size was measured to be in the range of 3–8 nm. In the FT-IR spectrum of CQDs, the peaks at 3415, 2931, and 1596 correspond to O—H, C—H, and COO$^-$ stretching vibrations, respectively. Also, the x-ray diffraction pattern of CQDs show a wide spectrum at $2\Theta = 20.75$ that correspond to the diffraction plane and indicated that the structure of CQDs was amorphous. Upon addition of METH, the fluorescence signal of the CQDs/SiO$_2$@ms-MIPs was enhanced. The results shows that the fluorescence intensity of MIPs was much more than NIPs. This is due to the presence of cavities that are designed for METH in the nanocomposite structure of MIPs. This method of detection was used to recognize METH in human plasma and urine samples achieving a detection level of 37 μM in urine and 42 μM in plasma.

Similarly, Hassanzadeh et al. [105] studied the sensitivity of fluorescence and chemiluminescence methods for recognition of METH using L-Cysteine capped CdS QDs in spiked urine samples. It was reported that the fluorescence properly of L-Cysteine capped CdS QDs have a robust boosting effect on the chemiluminescence emission of rhodamine B (RhoB)-cetyltrimethylammonium bromide (CTAB)-KMnO$_4$. Having prepared CdS QDs in-house, X-ray diffraction measured approximately 5 nm as average crystal size of CdS QDs. Using a blend of RhoB-CTAG-KMnO4-CdS QDs with chemiluminescence which enhanced the reaction with METH molecules. This showed a linear relationship with the concentration of METH. However, it was found that even trace amount of METH led to a notable decline in the fluorescence emission intensity of CdS QDs which relates to the absorption spectra of QDs being affected in presence of METH molecules which leads to a decrease in the emission of QDs. Therefore, a linear relationship between the concentration of METH and fluorescence intensity of QDs forms the basis of fluorometric determination of METH. Their results show detection limit of 1.8 μg/L and 0.086 μg/L in spiked urine samples for fluorescence and chemiluminescence methods, respectively.

Along similar lines of METH detection using fluorescence, Masteri-Farahani et al. [106] studied the effect of graphene quantum dots encapsulated within molecularly imprinted polymers (GQDs@MIP)

using fluorescence method. They studied properties of GQDs@MIP (see Fig. 11) in recognition of METH by recording the fluorescence spectra and various concentrations of METH from 0 to 50 μM were sequentially added to the sample solution and fluorescence spectra were recorded at each addition. They prepared the GQDs@MIP in-house which represents a fluorescence emission peak at 420 with excitation wavelength of 365 nm. The fluorescence intensity of GQDs@MIP greatly reduced when METH was introduced into the solution. Their method of using GQDs embedded within MIPs achieved a detection limit of 1.7 μg/mL.

In subsequent studies [107–109], Masteri-Farahani et al. further analyzed the use of quantum dots with a fluorescent probe for recognition of METH and at the same time, Saberi et al. [110] studied the effect of Cobalt oxyhydroxide (CoOOH) nanosheets as fluorescence quenchers in combination with Carbon Dots (CDs) due to their high surface area and specific optical properties. They presented an aptamer based fluorometric assay for recognition of METH, making use of fluorescent CDs that are conjugated to the aptamer. The role played by CoOOH is that of a quencher that reduces the fluorescence of the CDs. Their method yielded a detection limit of 3.2 nM in human plasma. Another study that incorporated fluorescence technique using Cadmium Selenide (CdSe) quantum dot nanoparticles for recognition of METH was carried out by Davoodi et al. [111]. Table 4 summarizes all the studies discussed on quantum dots. An image of graphene quantum dots is shown below:

3. Discussion and outlook

Consumption of illicit drugs and drug abuse is a global issue that needs both time and money to battle. Detection of illicit drugs is particularly of importance to the government and law enforcement agencies. Hence, it is prudent to investigate how detection of illicit substances can be achieved through various analytical methods. Plenty of research has been conducted in last several decades for recognition of illicit substances. There are numerous techniques of detecting substances of interest in many different sample matrices. METH and Cannabis are most widely used drugs. However, METH was chosen because of its obvious prevalence as the most abused drug in New Zealand and around the world. METH is consumed illegally through various forms of intake such as smoking, taking it orally in the form of power or inhaled, injecting into the blood stream, and snorted. Consumption of METH causes various health repercussions such as damage to the brain, erratic behavior, confusion, disruption to alertness, paranoia, stroke and even death.

Therefore, this review has presented a comprehensive analysis of various kinds of nanoparticle that have facilitated the recognition of METH through various detection techniques such as electrochemical, colorimetric, fluorescence, Raman spectroscopy, and solid phase extraction in various matrices such as human urine, saliva, plasma, and even wastewater. Most of the detection techniques were found to be
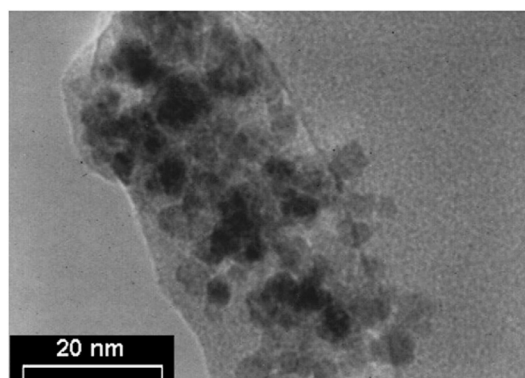

Fig. 11. TEM image of GQD@MIP [106].

Table 4
Quantum dot nanoparticle-based detection techniques.

Detection technique	Type of nanoparticle	Limit of detection	Detection time	Matrix type	Ref
Fluorescence	Carbon nanodots (CDs)	0.1 μg/mL	–	–	[103]
	Carbon quantum dots	1.6 μM (712 μg/mL)	–	Spiked urine	[104]
	Quantum dots	0.086 ng/mL	3 s	Spiked urine	[105]
	Graphene quantum dots	1.7 μg/mL	–	–	[106]
	CoOOH and CDs	3.2 nM (1.4 μg/mL)	–	Plasma	[110]
	CdSe quantum dots	0.15 nM (66 ng/mL)	–	Human urine	[111]
Electrochemical	Boron doped diamond	0.05 μM (22.25 μg/mL)	–	Human urine	[112]

based on colorimetric and fluorometric that rely on detecting color change as a result of aggregation of nanoparticles. Five different varieties of nanoparticles have come to light that focuses on recognition of METH. These are gold, silver, gold and silver core-shell, magnetic and quantum dots. Except for the types of nanoparticles mentioned above, no other varieties have come to light for METH detection. AuNPs have been found to be the most common choice for recognition of METH because of their ease of aggregation in the presence of target analyte that have been incorporated with analytical techniques such as electrochemistry, colorimetric and surface plasmon resonance. AuNPs have

been reported to amplify the detected signal [63], which facilitates in trace amounts of METH to be detected. The use of nanomaterials has enabled sensors to produce results rapidly with attributes like reproducibility and in some cases, also acted as a catalyst to aid oxidation and reduction of analyte [71]. A graphical summary representation of the limit of detection and detection times for some of the studies discussed in this review is shown in Fig. 12.

Several studies that have been analyzed in this review are laboratory based where results were obtained using expensive laboratory equipment such as transmission electron microscope (TEM), scanning electron microscope (SEM), ultraviolet-visible light spectrophotometer, fluorescence spectrometer, inductance-capacitance-resistance (LCR) meter, potentiostat-galvanostat, just to name a few. This requires specialized operating environment and trained personnel to operate the equipment. However, point of care methods or field-deployable systems are more desirable that would eliminate the need for special facilities and mitigates human intervention. To the best of our knowledge, only one study exists in the literature [100] that focuses on the development of method that is capable of field deployment. Therefore, further research is required around on-site detection of METH.

Field deployable drug detection systems are of great significance to interested government organizations. An ideal system would have a mechanism to take a sample, automatically analyze, and send the results to a remote computer for investigation, all carried out autonomously. An engineering approach for such a system could be of high value to interested parties. This kind of approach could be relevant and beneficial which would abide by some of the engineering parameters such as portability, fast response time, long life span, low cost and perhaps embeds some kind of IoT wireless technology without which human intervention would not be minimized. As shown in the diagram below, there are a few wireless technologies to choose from, with LoRa being widely used for communication over a long distance of a few hundred
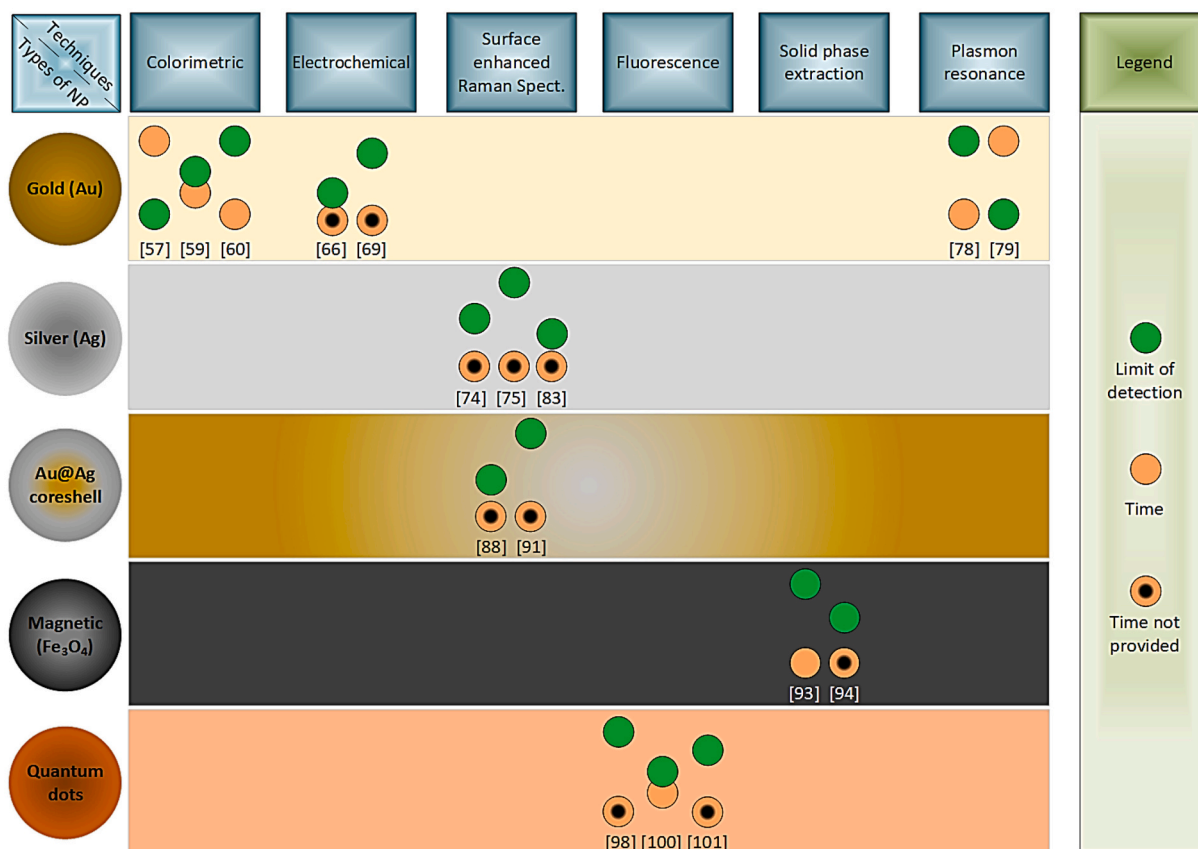
Fig. 12. Graphical representation of limit of detection and detection times for some of the studies discussed in this review.

meters and in some cases up to a kilometer of transmission within line of sight using an external antenna. However, it still suffers from a limited range when the system is deployed much further away. Which is where cellular technology comes in with technically no limit on communication distance, so long as there is cellular coverage available, the system can also be deployed in remote areas with options of overseas deployment. Communication with an independent system needs to be self-sustainable, reliable with fast data transfer rates and cellular technologies such as 4G and upcoming 5G, data transfer rates have never been better. Earlier generation communication technologies can also be used for low data rate applications. Sigfox is low-cost long battery life option

for light-weight message transfer from IoT devices to backend system. Sensors along with IoT communication provide a good tool for remote monitoring, however an independent system would need power, and so, a reasonable renewable source such as a solar panel with a battery management system would be ideal to keep the system operating for a long period of time.

Designing such a field deployable system would come with certain challenges that can be divided into two key aspects: the engineering aspect that focuses on the sensor parameters, and then there are challenges of detecting METH for a deployable system. A robust method needs to be used which could be built around well-established
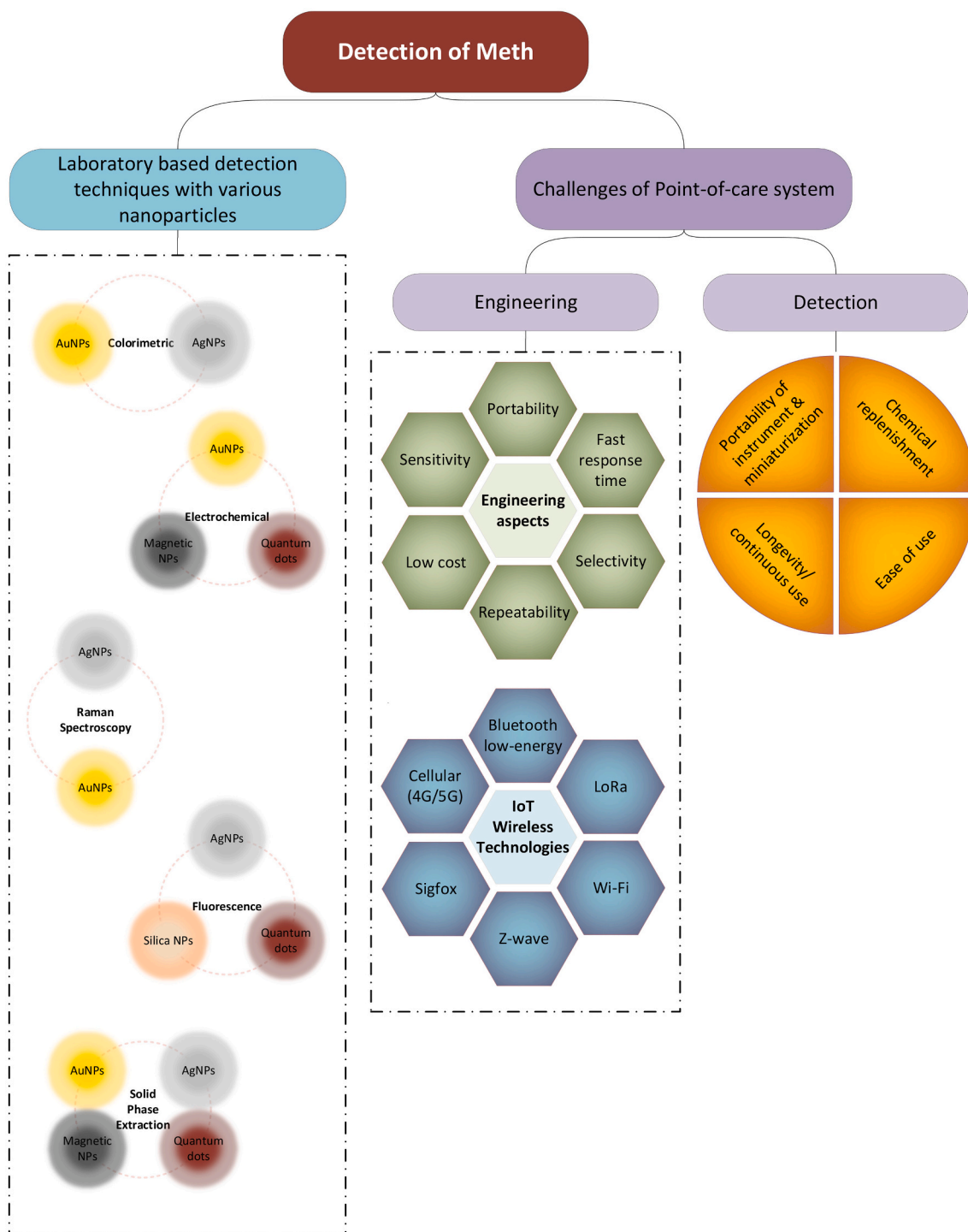

Fig. 13. Graphical representation of discussion and outlook.

laboratory-based methods that were discussed in this review. Hence, if gold nanoparticles are used, the system needs to be designed in such a way that would provide the qualities that are achievable from laboratory-based methods, yet at the same time miniaturized or portable which would be ideal for on-site analysis. Fig. 13 graphically illustrates the methods discussed in this review along with the challenges that come with a field deployable system.

Another approach to a field deployable system could be the installation of the system at the beginning of the wastewater pathway, i.e., toilets, sinks, and showers. Illicit drug detection system in miniaturized form could be placed in toilets and washbasins so that drugs could be detected at source. However, no such systems have been mentioned in the literature but the availability of smart toilets for huma health monitoring makes this approach a good candidate to adopt/explore.

There is an ongoing debate around disposable vs. reusable sensing systems, which equally applies to the discussion represented here. The choice of sensing system/mechanism normally relies on factors such as the cost and ease of deployment, which depends on how long a sensor can be used. For disposable systems a mechanism to replenish the cartridge (container) with individual sensors must be developed to allow independent monitoring over a period, especially if the deployment is at the beginning of the wastewater pathway. On the other hand, a reusable system can be easily deployed without as long as the sensor cleaning or other adjustments/calibrations can be done to maintain the accuracy and repeatability of the measurements.

4. Conclusion

In this review, we presented and discussed different detection techniques that have been combined with nanoparticles, synthesized from various materials for the detection of Methamphetamine in various sample matrices. We categorized these nanoparticles into several sections and the information from each material of nanoparticle was summed up in the form of a table. Overall, this review provides an insight into the progress of recognition of Methamphetamine with the use of different detection techniques combined with various nanoparticles. An engineering approach to the development of point of care system for the detection of Methamphetamine combined with IoT technologies ideal for remote monitoring of drug consumption has also been discussed.

Declaration of Competing Interest

The authors declare that they have no known competing financial interests or personal relationships that could have appeared to influence the work reported in this paper.

Data availability

No data was used for the research described in the article.

Acknowledgements

References

[1] T. Lundqvist, Cognitive consequences of cannabis use: comparison with abuse of stimulants and heroin with regard to attention, memory and executive functions, Pharmacol. Biochem. Behav. 81 (2) (2005) 319–330.

[2] D.W. Lachenmeier, J. Rehm, Comparative risk assessment of alcohol, tobacco, cannabis and other illicit drugs using the margin of exposure approach, Sci. Rep. 5 (1) (2015) 1–7.

[3] J.S. Lee, et al., Analysis of the impurities in the methamphetamine synthesized by three different methods from ephedrine and pseudoephedrine 161 (2–3) (2006) 209–215.

[4] C.S. Taylor, Dangerous Society, Michigan State University Press East Lansing, 1990.

[5] G.J.L.A.P. Duncan, Drug trafficking and political power: oligopolies of coercion in Colombia and Mexico 41 (2) (2014) 18–42.

[6] M. Gunnarsson, C. Fahlke, J.J.L. Balldin, Adolescents who have tried illicit drugs and experienced psychiatric symptoms seldom seek professional help. A pilot study of 18-year old high school students in an urban district 101 (14) (2004) 1280–1282.

[7] I.R. Edwards, J.K. Aronson, Adverse drug reactions: definitions, diagnosis, and management, Lancet 356 (9237) (2000) 1255–1259.

[8] M. Donaldson, J.H. Goodchild, Oral health of the methamphetamine abuser, Am. J. Health Syst. Pharm. 63 (21) (2006) 2078–2082.

[9] T.A. Wearne, J.L. Cornish, A comparison of methamphetamine-induced psychosis and schizophrenia: a review of positive, negative, and cognitive symptomatology, Frontiers in psychiatry (2018) 491.

[10] M.D. Prakash, et al., Methamphetamine: effects on the brain, gut and immune system, Pharmacol. Res. 120 (2017) 60–67.

[11] D.M. Stoneberg, R.K. Shukla, M.B. Magness, Global methamphetamine trends: an evolving problem, International Criminal Justice Review 28 (2) (2018) 136–161.

[12] U. Drugs, M. Crime, World drug report 2010, United Nations Publications New York, 2010.

[13] I. Nestorov, Whole body pharmacokinetic models, Clin. Pharmacokinet. 42 (10) (2003) 883–908.

[14] P. Sharma, P. Murthy, M.S. Bharath, Chemistry, metabolism, and toxicology of cannabis: clinical implications, Iran. J. Psychiatry 7 (4) (2012) 149.

[15] S.I. Johannessen, T. Tomson, Pharmacokinetic variability of newer antiepileptic drugs, Clin. Pharmacokinet. 45 (11) (2006) 1061–1075.

[16] M.A. Hughes, P. Glass, J.R. Jacobs, Context-sensitive half-time in multicompartment pharmacokinetic models for intravenous anesthetic drugs, Anesthesiology 76 (3) (1992) 334–341.

[17] D.E. Mager, W.J. Jusko, General pharmacokinetic model for drugs exhibiting target-mediated drug disposition, J. Pharmacokinet. Pharmacodyn. 28 (6) (2001) 507–532.

[18] N. Shima, et al., Urinary excretion of the main metabolites of methamphetamine, including p-hydroxymethamphetamine-sulfate and p-hydroxymethamphetamine-glucuronide, in humans and rats, Xenobiotica 36 (2–3) (2006) 259–267.

[19] J. Caldwell, L. Dring, R. Williams, Metabolism of [14C] methamphetamine in man, the guinea pig and the rat, Biochem. J. 129 (1) (1972) 11–22.

[20] R.O. Hughes, W.E. Bronner, M.L. Smith, Detection of amphetamine and methamphetamine in urine by gas chromatography/mass spectrometry following derivatization with (−)-menthyl chloroformate, J. Anal. Toxicol. 15 (5) (1991) 256–259.

[21] P. Lebish, B.S. Finkle, J. Brackett Jr., Determination of amphetamine, methamphetamine, and related amines in blood and urine by gas chromatography with hydrogen-flame ionization detector, Clin. Chem. 16 (3) (1970) 195–200.

[22] S.-W. Myung, et al., Determination of amphetamine, methamphetamine and dimethamphetamine in human urine by solid-phase microextraction (SPME)-gas chromatography/mass spectrometry, J. Chromatogr. B Biomed. Sci. Appl. 716 (1–2) (1998) 359–365.

[23] H. Bagheri, A.F. Zavareh, M.H. Koruni, Graphene oxide assisted electromembrane extraction with gas chromatography for the determination of methamphetamine as a model analyte in hair and urine samples, J. Sep. Sci. 39 (6) (2016) 1182–1188.

[24] J.T. Cody, Determination of methamphetamine enantiomer ratios in urine by gas chromatography—mass spectrometry, J. Chromatogr. B Biomed. Sci. Appl. 580 (1–2) (1992) 77–95.

[25] T. Kumazawa, et al., Simultaneous determination of methamphetamine and amphetamine in human urine using pipette tip solid-phase extraction and gas chromatography–mass spectrometry, J. Pharm. Biomed. Anal. 44 (2) (2007) 602–607.

[26] H. Kataoka, H.L. Lord, J. Pawliszyn, Simple and rapid determination of amphetamine, methamphetamine, and their methylenedioxy derivatives in urine by automated in-tube solid-phase microextraction coupled with liquid chromatography-electrospray ionization mass spectrometry, J. Anal. Toxicol. 24 (4) (2000) 257–265.

[27] M.-R. Fuh, T.-Y. Wu, T.-Y. Lin, Determination of amphetamine and methamphetamine in urine by solid phase extraction and ion-pair liquid chromatography–electrospray–tandem mass spectrometry, Talanta 68 (3) (2006) 987–991.

[28] Y. He, Y.-J. Kang, Single drop liquid–liquid–liquid microextraction of methamphetamine and amphetamine in urine, J. Chromatogr. A 1133 (1–2) (2006) 35–40.

[29] M.S. Tehrani, M.H. Givianrad, N. Mahoor, Surfactant-assisted dispersive liquid–liquid microextraction followed by high-performance liquid chromatography for determination of amphetamine and methamphetamine in urine samples, Anal. Methods 4 (5) (2012) 1357–1364.

[30] R. Wang, et al., Ionic-liquid-based dispersive liquid–liquid microextraction coupled with high-performance liquid chromatography for the forensic determination of methamphetamine in human urine, J. Sep. Sci. 39 (13) (2016) 2444–2450.

[31] A. Taghvimi, H. Hamishehkar, M. Ebrahimi, The application of magnetic nano graphene oxide in determination of methamphetamine by high performance liquid chromatography of urine samples, J. Iran. Chem. Soc. 13 (8) (2016) 1471–1480.

[32] M. Kumihashi, et al., Simultaneous determination of methamphetamine and its metabolite, amphetamine, in urine using a high performance liquid chromatography column-switching method, J. Chromatogr. B 845 (1) (2007) 180–183.

[33] K. Hayakawa, et al., Simultaneous determination of methamphetamine and its metabolites in the urine samples of abusers by high performance liquid chromatography with chemiluminescence detection, Biol. Pharm. Bull. 16 (9) (1993) 817–821.

[34] K. Hayakawa, et al., Determination of methamphetamine, amphetamine and piperidine in human urine by high-performance liquid chromatography with chemiluminescence detection, J. Chromatogr. A 515 (1990) 459–466.

[35] O. Al-Dirbashi, et al., Enantioselective high-performance liquid chromatography with fluorescence detection of methamphetamine and its metabolites in human urine, Analyst 123 (11) (1998) 2333–2337.

[36] N. Kato, et al., Thin layer chromatography/fluorescence detection of 3, 4-methylenedioxy-methamphetamine and related compounds 53 (6) (2008) 1367–1371.

[37] K. Fekri, et al., Comparison of High-Performance Liquid Chromatography and Thin Layer Chromatography for Identification of Amphetamine and Methamphetamine in Human Urine 1 (1) (2018) 24–28.

[38] J. Klimes, P.J.C.a.S.f.c.C.f.s.a.S.f.s. Pilarova, Thin-layer chromatography analysis of methamphetamine in urine samples 45 (6) (1996) 279–283.

[39] M. Akhgari, et al., Forensic laboratory validation of immunochromatography and gas chromatography/mass spectrometry methods for the detection of methamphetamine and amphetamine in postmortem urine specimens 33 (2) (2021) 109–115.

[40] T. Mikuma, et al., The use of a sulfonated capillary on chiral capillary electrophoresis/mass spectrometry of amphetamine-type stimulants for methamphetamine impurity profiling 249 (2015) 59–65.

[41] J. Zhai, H. Cui, R.J.B.A. Yang, DNA based biosensors 15 (1) (1997) 43–58.

[42] T. Ohmichi, et al., DNA-based biosensor for monitoring pH in vitro and in living cells 44 (19) (2005) 7125–7130.

[43] G. Marko-Varga, K. Johansson, L. Gorton, Enzyme-based biosensor as a selective detection unit in column liquid chromatography, J. Chromatogr. A 660 (1–2) (1994) 153–167.

[44] N. Maleki, et al., A novel enzyme based biosensor for catechol detection in water samples using artificial neural network 128 (2017) 1–11.

[45] G.S. Wilson, Y.J.C.R. Hu, Enzyme-based biosensors for in vivo measurements 100 (7) (2000) 2693–2704.

[46] K. Yagiuda, et al., Development of a conductivity-based immunosensor for sensitive detection of methamphetamine (stimulant drug) in human urine 11 (8) (1996) 703–707.

[47] G. Sakai, et al., Highly selective and sensitive SPR immunosensor for detection of methamphetamine 44 (21−22) (1999) 3849–3854.

[48] N. Miura, et al., Piezoelectric crystal immunosensor for sensitive detection of methamphetamine (stimulant drug) in human urine 13 (1–3) (1993) 188–191.

[49] S. Shukla, P. Govender, A. Tiwari, Polymeric micellar structures for biosensor technology, in: Advances in Biomembranes and Lipid Self-Assembly, Elsevier, 2016, pp. 143–161.

[50] K. Nishio, et al., Preparation of size-controlled (30–100 nm) magnetite nanoparticles for biomedical applications, J. Magn. Magn. Mater. 310 (2) (2007) 2408–2410.

[51] M. Shao, et al., Electrochemical surface area measurements of platinum-and palladium-based nanoparticles, Electrochem. Commun. 31 (2013) 46–48.

[52] Y.-C. Yeh, B. Creran, V.M. Rotello, Gold nanoparticles: preparation, properties, and applications in bionanotechnology, Nanoscale 4 (6) (2012) 1871–1880.

[53] R. Sardar, et al., Gold nanoparticles: past, present, and future, Langmuir 25 (24) (2009) 13840–13851.

[54] D. Cabuzu, et al., Biomedical applications of gold nanoparticles, Curr. Top. Med. Chem. 15 (16) (2015) 1605–1613.

[55] M.L. Firdaus, et al., Smartphone-based digital image colorimetry for non-enzymatic detection of glucose using gold nanoparticles, Sensing and Bio-Sensing Research 35 (2022), 100472.

[56] Y. Zhang, et al., New gold nanostructures for sensor applications: a review, Materials 7 (7) (2014) 5169–5201.

[57] Y. Zhang, et al., Multifunctional gold nanorods with ultrahigh stability and tunability for in vivo fluorescence imaging, SERS detection, and photodynamic therapy, Angew. Chem. Int. Ed. 52 (4) (2013) 1148–1151.

[58] G. Liu, et al., Application of gold-nanoparticle colorimetric sensing to rapid food safety screening, Sensors 18 (12) (2018) 4166.

[59] Q. Shi, et al., Colorimetric and bare eye determination of urinary methylamphetamine based on the use of aptamers and the salt-induced aggregation of unmodified gold nanoparticles, Microchim. Acta 182 (3) (2015) 505–511.

[60] L. Wang, et al., Unmodified gold nanoparticles as a colorimetric probe for potassium DNA aptamers, Chem. Commun. 36 (2006) 3780–3782.

[61] M. Yarbakht, M. Nikkhah, Unmodified gold nanoparticles as a colorimetric probe for visual methamphetamine detection, J. Exp. Nanosci. 11 (7) (2016) 593–601.

[62] K. Mao, et al., Rapid duplexed detection of illicit drugs in wastewater using gold nanoparticle conjugated aptamer sensors, Sci. Total Environ. 688 (2019) 771–779.

[63] O. Adegoke, et al., Biomimetic graphene oxide-cationic multi-shaped gold nanoparticle-hemin hybrid nanozyme: tuning enhanced catalytic activity for the rapid colorimetric apta-biosensing of amphetamine-type stimulants, Talanta 216 (2020), 120990.

[64] H.L. Zou, et al., A novel electrochemical biosensor based on hemin functionalized graphene oxide sheets for simultaneous determination of ascorbic acid, dopamine and uric acid, Sensors Actuators B Chem. 207 (2015) 535–541.

[65] T. Zhang, et al., Hemin immobilized into metal–organic frameworks as an electrochemical biosensor for 2, 4, 6-trichlorophenol, Nanotechnology 29 (7) (2018) 074003.

[66] L. Shaw, L. Dennany, Applications of electrochemical sensors: forensic drug analysis, Current Opinion in Electrochemistry 3 (1) (2017) 23–28.

[67] C.-H. Yeh, et al., A developed competitive immunoassay based on impedance measurements for methamphetamine detection, Microfluid. Nanofluid. 13 (2) (2012) 319–329.

[68] M. Alijanianzadeh, F. Qadami, A. Molaeirad, Detection of methamphetamine using aptamer-based biosensor chip and cyclic voltammetry technique, J. Indian Chem. Soc. 98 (11) (2021), 100189.

[69] M. Ebrahimi, et al., Electrochemical impedance spectroscopic sensing of methamphetamine by a specific aptamer, BioImpacts: BI 2 (2) (2012) 91.

[70] B. Rafiee, A.R. Fakhari, M. Ghaffarzadeh, Impedimetric and stripping voltammetric determination of methamphetamine at gold nanoparticles-multiwalled carbon nanotubes modified screen printed electrode, Sensors Actuators B Chem. 218 (2015) 271–279.

[71] M. Haghighi, et al., New and sensitive sensor for voltammetry determination of methamphetamine in biological samples, J. Mater. Sci. Mater. Electron. 31 (14) (2020) 10989–11000.

[72] L.A. Lyon, et al., Raman spectroscopy, Anal. Chem. 70 (12) (1998) 341–362.

[73] D. Maddipatla, et al., Development of a novel wrinkle-structure based SERS substrate for drug detection applications, Sensing and Bio-Sensing Research 24 (2019), 100281.

[74] R.R. Jones, et al., Raman techniques: fundamentals and frontiers, Nanoscale Res. Lett. 14 (1) (2019) 1–34.

[75] Y. Ma, et al., Surface-enhanced Raman spectroscopy on liquid interfacial nanoparticle arrays for multiplex detecting drugs in urine, Anal. Chem. 88 (16) (2016) 8145–8151.

[76] Y. Hong, et al., Optoplasmonic hybrid materials for trace detection of methamphetamine in biological fluids through SERS, ACS Appl. Mater. Interfaces 12 (21) (2020) 24192–24200.

[77] J. Mao, et al., Surface-enhanced Raman spectroscopy integrated with aligner mediated cleavage strategy for ultrasensitive and selective detection of methamphetamine, Anal. Chim. Acta 1146 (2021) 124–130.

[78] W. Fang, et al., On-site and quantitative detection of trace methamphetamine in urine/serum samples with a surface-enhanced Raman scattering-active microcavity and rapid pretreatment device, Anal. Chem. 92 (19) (2020) 13539–13549.

[79] R. Kohzadi, et al., Designing a label free aptasensor for detection of methamphetamine, Biom. J. 2 (1) (2016) 28–33.

[80] M.R. Guerra, et al., Development of a piezoelectric sensor for the detection of methamphetamine, Analyst 134 (8) (2009) 1565–1570.

[81] T.-C. Chang, et al., Fiber optic particle plasmon resonance immunosensor for rapid and sensitive detection of methamphetamine based on competitive inhibition, Microchem. J. 157 (2020), 105026.

[82] F. Qadami, et al., Localized surface plasmon resonance (LSPR)-based nanobiosensor for methamphetamin measurement, Plasmonics 13 (6) (2018) 2091–2098.

[83] S. Weng, et al., Dynamic surface-enhanced Raman spectroscopy and Chemometric methods for fast detection and intelligent identification of methamphetamine and 3, 4-Methylenedioxy methamphetamine in human urine, Spectrochim. Acta A Mol. Biomol. Spectrosc. 189 (2018) 1–7.

[84] B. Li, et al., Fabrication of au nanorods by the oblique angle deposition process for trace detection of methamphetamine with surface-enhanced Raman scattering, Sensors 19 (17) (2019) 3742.

[85] Y. Hong, et al., Engineered optoplasmonic core-satellite microspheres for SERS determination of methamphetamine derivative and its precursors, Sensors and Actuators B: Chemical (2022) 131437.

[86] K. Varghese Alex, et al., Green synthesized ag nanoparticles for bio-sensing and photocatalytic applications, ACS omega 5 (22) (2020) 13123–13129.

[87] A. Loiseau, et al., Silver-based plasmonic nanoparticles for and their use in biosensing, Biosensors 9 (2) (2019) 78.

[88] M.A. Souza, et al., The adsorption of methamphetamine on ag nanoparticles dispersed in agarose gel–detection of methamphetamine in fingerprints by SERS, Vib. Spectrosc. 98 (2018) 152–157.

[89] R. Salemmilani, et al., Dielectrophoretic nanoparticle aggregation for on-demand surface enhanced raman spectroscopy analysis, Anal. Chem. 90 (13) (2018) 7930–7936.

[90] C. Andreou, et al., Rapid detection of drugs of abuse in saliva using surface enhanced Raman spectroscopy and microfluidics, ACS Nano 7 (8) (2013) 7157–7164.

[91] K. Okajima, et al., Highly sensitive analysis of methamphetamine and amphetamine in human whole blood using headspace solid-phase microextraction and gas chromatography–mass spectrometry, Forensic Sci. Int. 116 (1) (2001) 15–22.

[92] K. Mao, et al., A novel biosensor based on au@ ag core-shell nanoparticles for sensitive detection of methylamphetamine with surface enhanced Raman scattering, Talanta 190 (2018) 263–268.

[93] K. Mao, et al., A novel colorimetric biosensor based on non-aggregated au@ ag core–shell nanoparticles for methamphetamine and cocaine detection, Talanta 175 (2017) 338–346.

[94] K. Mao, et al., Based nanosensors to evaluate community-wide illicit drug use for wastewater-based epidemiology, Water Res. 189 (2021), 116559.

[95] N.D. Kline, et al., Optimization of surface-enhanced Raman spectroscopy conditions for implementation into a microfluidic device for drug detection, Anal. Chem. 88 (21) (2016) 10513–10522.

[96] V. Riahifar, et al., A sensitive voltammetric sensor for methamphetamine determination based on modified glassy carbon electrode using Fe3O4@ poly pyrrole core-shell and graphene oxide, Microchem. J. 170 (2021), 106748.

[97] S.A. Haeri, S. Abbasi, S. Sajjadifar, Bio-dispersive liquid liquid microextraction based on nano rhaminolipid aggregates combined with magnetic solid phase extraction using Fe3O4@ PPy magnetic nanoparticles for the determination of methamphetamine in human urine, J. Chromatogr. B 1063 (2017) 101–106.

[98] A. Taghvimi, S. Dastmalchi, Y. Javadzadeh, Novel ceramic carbon-coated magnetic nanoparticles as stir bar sorptive extraction coating for simultaneous extraction of amphetamines from urine samples, Arab. J. Sci. Eng. 44 (7) (2019) 6373–6380.

[99] K. Icoz, B.D. Iverson, C. Savran, Noise analysis and sensitivity enhancement in immunomagnetic nanomechanical biosensors, Appl. Phys. Lett. 93 (10) (2008), 103902.

[100] G. Yang, et al., A miniaturized giant magnetic resistance system for quantitative detection of methamphetamine, Analyst 146 (8) (2021) 2718–2725.

[101] S.Y. Lim, W. Shen, Z. Gao, Carbon quantum dots and their applications, Chem. Soc. Rev. 44 (1) (2015) 362–381.

[102] Z. Liu, et al., Photoluminescence of carbon quantum dots: coarsely adjusted by quantum confinement effects and finely by surface trap states, SCIENCE CHINA Chem. 61 (4) (2018) 490–496.

[103] T.H. Kim, et al., Amine-rich carbon nanodots as a fluorescence probe for methamphetamine precursors, Anal. Methods 7 (16) (2015) 6869–6876.

[104] S. Mandani, B. Rezaei, A.A. Ensafi, Sensitive imprinted optical sensor based on mesoporous structure and green nanoparticles for the detection of methamphetamine in plasma and urine, Spectrochim. Acta A Mol. Biomol. Spectrosc. 231 (2020), 118077.

[105] J. Hassanzadeh, A. Khataee, R. Lotfi, Sensitive fluorescence and chemiluminescence procedures for methamphetamine detection based on CdS quantum dots, Microchem. J. 132 (2017) 371–377.

[106] M. Masteri-Farahani, S. Mashhadi-Ramezani, N. Mosleh, Molecularly imprinted polymer containing fluorescent graphene quantum dots as a new fluorescent nanosensor for detection of methamphetamine, Spectrochim. Acta A Mol. Biomol. Spectrosc. 229 (2020), 118021.

[107] M. Masteri-Farahani, N. Mosleh, Modified CdS quantum dots as selective turn-on fluorescent nanosensor for detection and determination of methamphetamine, J. Mater. Sci. Mater. Electron. 30 (24) (2019) 21170–21176.

[108] M. Masteri-Farahani, et al., L-and D-cysteine functionalized CdS quantum dots as nanosensors for detection of L-morphine and D-methamphetamine, Journal of Nanostructures 8 (4) (2018) 325–331.

[109] M. Masteri-Farahani, F. Askari, Design and photophysical insights on graphene quantum dots for use as nanosensor in differentiating methamphetamine and morphine in solution, Spectrochim. Acta A Mol. Biomol. Spectrosc. 206 (2019) 448–453.

[110] Z. Saberi, et al., A fluorometric aptasensor for methamphetamine based on fluorescence resonance energy transfer using cobalt oxyhydroxide nanosheets and carbon dots, Microchim. Acta 185 (6) (2018) 1–10.

[111] M. Davoodi, et al., CdSe quantum dot nanoparticles: synthesis and application in the development of molecularly imprinted polymer-based dual optical sensors, Ind. Eng. Chem. Res. 60 (33) (2021) 12328–12342.

[112] Ľ. Švorc, et al., Electrochemical behavior of methamphetamine and its voltammetric determination in biological samples using self-assembled boron-doped diamond electrode, J. Electroanal. Chem. 717 (2014) 34–40.

Methamphetamine detection using nanoparticle-based biosensors: A comprehensive review

Lal, K

2022-10-25